

Systematics, endemism and phylogeny of Indian proplanulitins (Ammonoidea) from the Bathonian–Callovian of Kutch, western India

Rakhi Dutta¹ · Subhendu Bardhan¹

Received: 25 February 2015 / Accepted: 28 August 2015 / Published online: 8 December 2015
© Akademie der Naturwissenschaften Schweiz (SCNAT) 2015

Abstract Spath (1931) described five genera namely *Sivajicerias* Spath, *Obtusicosites* Buckman, *Hubertoceras* Spath, *Kinkeliniceras* Buckman and *Cutchisphinctes* Spath from the Upper Bathonian and entire Callovian of Kutch, western India and included 33 species within them. He grouped these genera within the subfamily Proplanulitinae of the Boreal Province. But however the palaeobiogeographic distributions of the Kutch forms suggest that they were restricted within the Indo-Madagascan Province. Callomon (1993) expressed doubts about the phylogenetic affinity of Kutch genera and inferred that proplanulitins of Kutch were unrelated to Boreal *Proplanulites* and constitute an endemic lineage. In the present study, we made a thorough systematic revision of proplanulitin taxa of Kutch in the light of intraspecific variability and sexual dimorphism. Our study reveals that Spath's (1931) work suffered from excessive and subjective splitting. Many species described by him were nothing but variants of a single, variable, biological species. The genus *Hubertoceras* was considered as the microconch of *Obtusicosites*. *Cutchisphinctes* was excluded as it appears to be unrelated. We finally described two species within each genus, *Sivajicerias*, *Obtusicosites* and *Kinkeliniceras* from the Callovian. We grouped these Kutch genera within a new subfamily Sivajiceratinae which is distinct from the existing subfamily Proplanulitinae. The oldest genus *Sivajicerias* evolved from contemporary *Procerites* during the Late

Bathonian of Kutch (Roy et al. 2007). *Procerites* was a European genus and perhaps gave rise to *Proplanulites* in the Boreal Europe. We here envisaged that Sivajiceratinae and the European Proplanulitinae show evolutionary convergence of some characters since they evolved from a common ancestral stock.

Keywords Sivajiceratinae · New subfamily · Kutch · Middle Jurassic · Palaeobiogeography · Evolution

Introduction

The Bathonian of Kutch, western India, witnessed sudden migration of many ammonite genera from different provinces as soon as the Kutch Basin opened up (Roy et al. 2007). Macrocephalitins, for example, invaded from the West Pacific Province (Indonesia) and underwent a spectacular radiation of many endemic genera/species during Late Bathonian–Early Callovian times (Spath 1931). Five genera namely *Sivajicerias* Spath, *Obtusicosites* Buckman, *Hubertoceras* Spath, *Kinkeliniceras* Buckman and *Cutchisphinctes* Spath were described by Spath (1931) from the Upper Bathonian to entire Callovian successions of Kutch. All these genera were new records in Kutch and grouped within the subfamily of Proplanulitinae of the Boreal Province. Since their first description, the new genera were continuously referred to as proplanulitins although their paleobiogeographic occurrence was restricted to the Indo-Madagascan Province and not a single species of the Boreal genus *Proplanulites* has been recorded from Kutch or neighbouring regions. It was Callomon (1993) who first expressed doubts about the phylogenetic affinity of Kutch genera and predicted that a detailed study would one day reveal that Kutch proplanulitins are entirely

✉ Rakhi Dutta
rakhi.geol@gmail.com

Subhendu Bardhan
sbardhan12@gmail.com

¹ Department of Geological Sciences, Jadavpur University, Kolkata 700032, India

unrelated to the Boreal forms and constitute an endemic lineage.

In the present study, we revisited Kutch's the so-called proplanulitins. Our study included type material archived in the Geological Survey of India, Kolkata; The Natural History Museum, U.K. and numerous additional specimens collected by us from different sections in the mainland of the Kutch Basin with precise stratigraphic information. We studied the group in the light of new information on intraspecific variability and sexual dimorphism within a biological species. The concept of sexual dimorphism was not in vogue during the time of Spath (1931). The detailed systematic revision led to synonymising many of the Spath's species into a single species. Dimorphism has been established in most of the species. These revised endemic genera were assigned to a new subfamily Sivajiceratinae n. subfam. We excluded another genus *Cutchisphinctes* described by Spath (1931) because it shows strong resemblance to the subfamily Pseudoperisphinctinae, more specifically to *Choffatia*.

Roy et al. (2007) made an attempt to establish the evolutionary relationship between the older *Procerites* which was found in the Bathonian of Kutch and the contemporaneous *Sivajicerates*, the type genus of the new subfamily Sivajiceratinae. We will reiterate their view regarding the origin of the Sivajiceratinae in the following and provide detailed evidence. We will try to explain the stunning similarities between the Boreal *Proplanulites* and the taxa from Kutch.

Geological setting

The origin of the Kutch Basin was related to the fragmentation of Gondwana during the Late Triassic to Early Jurassic. The exposed Jurassic sediments range in age from the Bajocian to Tithonian (Biswas 1982, 1991; Roy et al. 2007; Fürsich et al. 1994, 2013) and were deposited during repeated episodes of marine transgression and regression (see Biswas 1991; Mukherjee 2007). The fossiliferous Bathonian–Callovian sediments are exposed best in the mainland of Kutch, particularly in Jara, Jumara, Keera and Jhura in the NW of Bhuj, the principal district town of Kutch as well as in Ler-Fakirwadi, south of Bhuj (Fig. 1). These areas form domal outcrops (Mitra et al. 1979) due to subsequent tectonic activity and offer excellent sections.

All type specimens of the present new subfamily come from different localities of the mainland of Kutch (Waagen 1875; Spath 1931) (Fig. 1). In our extensive and repeated field surveys, we collected additional specimens mainly from Jumara and Keera. The Middle and Upper Bathonian sediments belong to the Patcham Formation while Callovian sediments are grouped into the Chari Formation (Mitra et al. 1979). The Patcham Formation in mainland is exposed only in Jumara and the Chari Formation is well exposed in many localities within mainland (Fig. 1). The biostratigraphy of Patcham and Chari formations are delineated by many workers in a series of previous studies (Mitra et al. 1979; Datta 1992; Roy et al. 2007). The depositional environment of the Patcham Formation was a

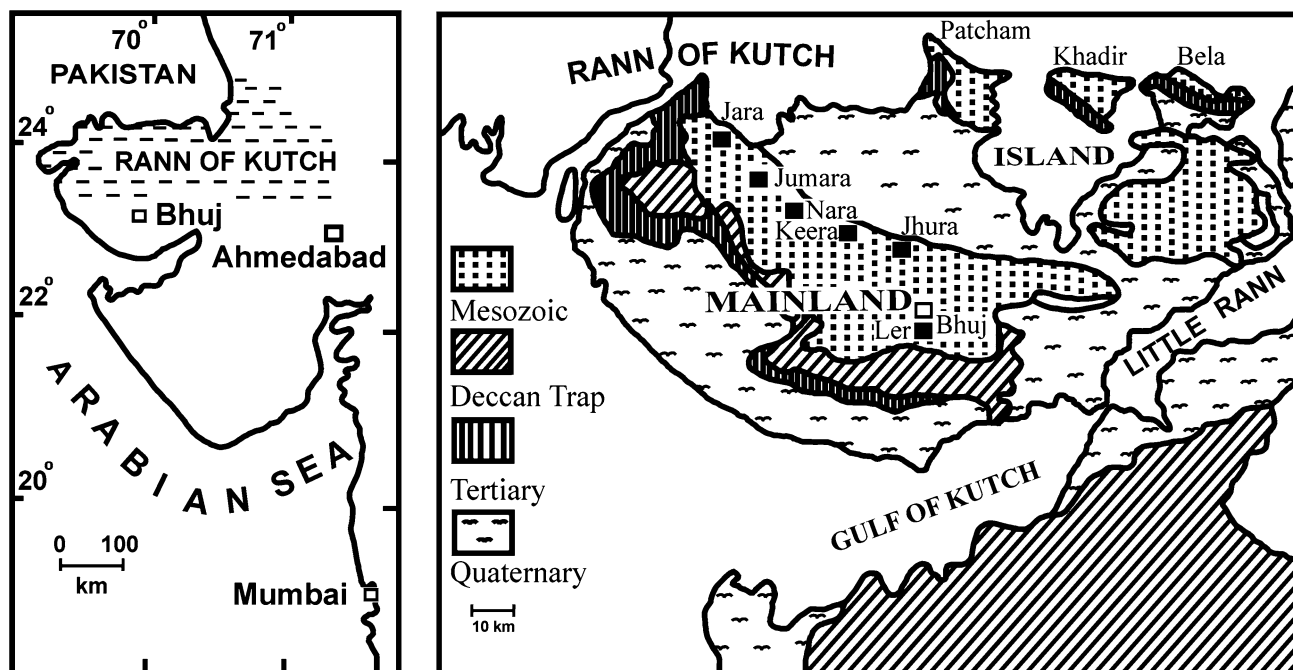


Fig. 1 Geological map of Kutch showing the major localities (solid squares) from where fossils of the Sivajiceratinae have been collected (modified after Biswas 1977; Fürsich and Pandey 2003)

carbonate ramp on the epicontinental shelf. The Upper Bathonian sediments in Jumara consist mainly of greenish to grey shale intercalated with shelly and white limestone of varying thickness (Roy et al. 2007). The depositional milieu of the Chari Formation was a shelf environment. The lower part of the Chari Formation is Early Callovian in age and includes mostly shale-limestone association (packstone or wackestone). The Middle Callovian beds are dominantly siliciclastic and represent a shoaling upward phase (Datta 1992; Fürsich and Oschmann 1993). The Upper Callovian beds are composed of an alternation between greenish grey shale, occasionally gypseous with secondary gypsum and white fossiliferous limestone. Dominantly, argillaceous facies in the Chari Formation were deposited in the outer ramp formed within the Kutch embayment (Fürsich et al. 2004). The sediments were deposited below storm wave base in low-energy environment.

The stratigraphic distributions of the studied genera of the Sivajiceratinae n. subfam., *Procerites* and other important ammonite species reported from the two studied localities (Jumara and Keera) are shown in Figs. 2 and 3. The stratigraphic distribution of these genera is shown in Fig. 4 against the regional biostratigraphic background.

Materials and methods

Our study material includes type specimens and own collections. The type material (no. of specimens = 40) of Waagen (1875) and Spath (1931) is archived in the repository of the Geological Survey of India, Kolkata and Natural History Museum, U.K. and most of it has been studied and photographed by us. The type specimens of Waagen (1875) were mostly collected from the golden oolite (Bed no. 2) and several other beds (Bed no. 5–8) of Keera. Only one specimen of the Bathonian *Sivajicerias* was collected by Waagen (1875) but we have collected additional specimens of the Sivajiceratinae from the Callovian of Jumara (Bed no. 7–13). Spath (1931) collected most of the types from Fakirwadi and Keera. For a comparison, we consulted literature including Waagen (1875), Buckman (1921), Spath (1931), Imlay (1962), Hahn (1969), Callomon (1993), Repin and Rashvan (1996a, b), Cariou et al. (1996), Cariou and Hantzergue (1997), Gulyaev (2001), Roy et al. (2007) etc. We conducted several field trips to collect many additional new specimens ($n = 64$) systematically with precise stratigraphic information from different sections of Kutch. Detailed morphological studies, measurements of data with electronic callipers and bivariate analyses have been made.

Systematic palaeontology

Abbreviations Specimen numbers bear the following repository institutional prefixes: NHMUK—Natural History Museum, United Kingdom; GSI—Geological Survey of India; Kolkata; JUM—Jadavpur University Museum-Kolkata (where all additional specimens are archived). * in front of the publication year in the synonymy list for the name-giving citation. v—in the synonymy list in front of the publication year indicates the specimens which were investigated in the present study. [M] and [m] designate macroconch and microconch, respectively. The following letters are used to indicate shell parameters: *D*—diameter of the shell; *U*—diameter of the umbilicus; *W*—width of the whorl; *H*—height of the whorl from the umbilical margin; *P*—number of primary ribs per half whorl; *S*—number of ventral ribs (secondary plus intercalatory ribs) per half whorl; *RW*—rib width of the shell; *RS*—rib space of the shell. *SP*—*Sivajicerias paramorphum*; *OO*—*Obtusicosites obtusica*; *KA*—*Kinkeliniceras angygaster*; *KK*—*Kinkeliniceras kinkelini*, *K*—Keera and *J*—Jumara.

Superfamily Perisphinctoidea Steinmann, 1890

Family Perisphinctidae Steinmann, 1890

Subfamily **Sivajiceratinae nov. subfam.**

Type genus: *Sivajicerias* Spath, 1930

Diagnosis: Shell large and evolute. Depressed inner whorls have strong, dense primary ribs. Secondary ribs are longer and furcate near the middle part of the flank. Phragmocone of macroconch with characteristic bullae-like primary ribs. Body whorl compressed and occupies half or 2/3rd of the outer whorl. Septal sutural patterns complex. Strongly dimorphic, microconch lappeted, evolute and strongly ribbed. The subfamily evolved from *Procerites* through complex heterochronic process. Endemic to Indo-Madagascan Faunal Province. The phragmocone of macroconchs superficially resembles that of *Proplanulites* in having bullae-like primary ribs. But the present subfamily has strong, dense primary ribs on inner whorls and complex suture. It differs from *Pseudoperisphinctinae* in having longer secondary ribs and nature of dimorphism.

Genera included: *Sivajicerias*, *Obtusicosites* and *Kinkeliniceras*.

Stratigraphical and geographical occurrences: Upper Bathonian to entire Callovian; Indo-Madagascan Faunal Province.

Genus ***Sivajicerias*** Spath, 1930

Type species: *Perisphinctes congener* Waagen 1875

Diagnosis: Macroconchiate shell very large (maximum $D = 204$ mm), highly evolute ($U/D = 0.35–0.53$), phragmocone with less bullae-like primaries, body whorl marked

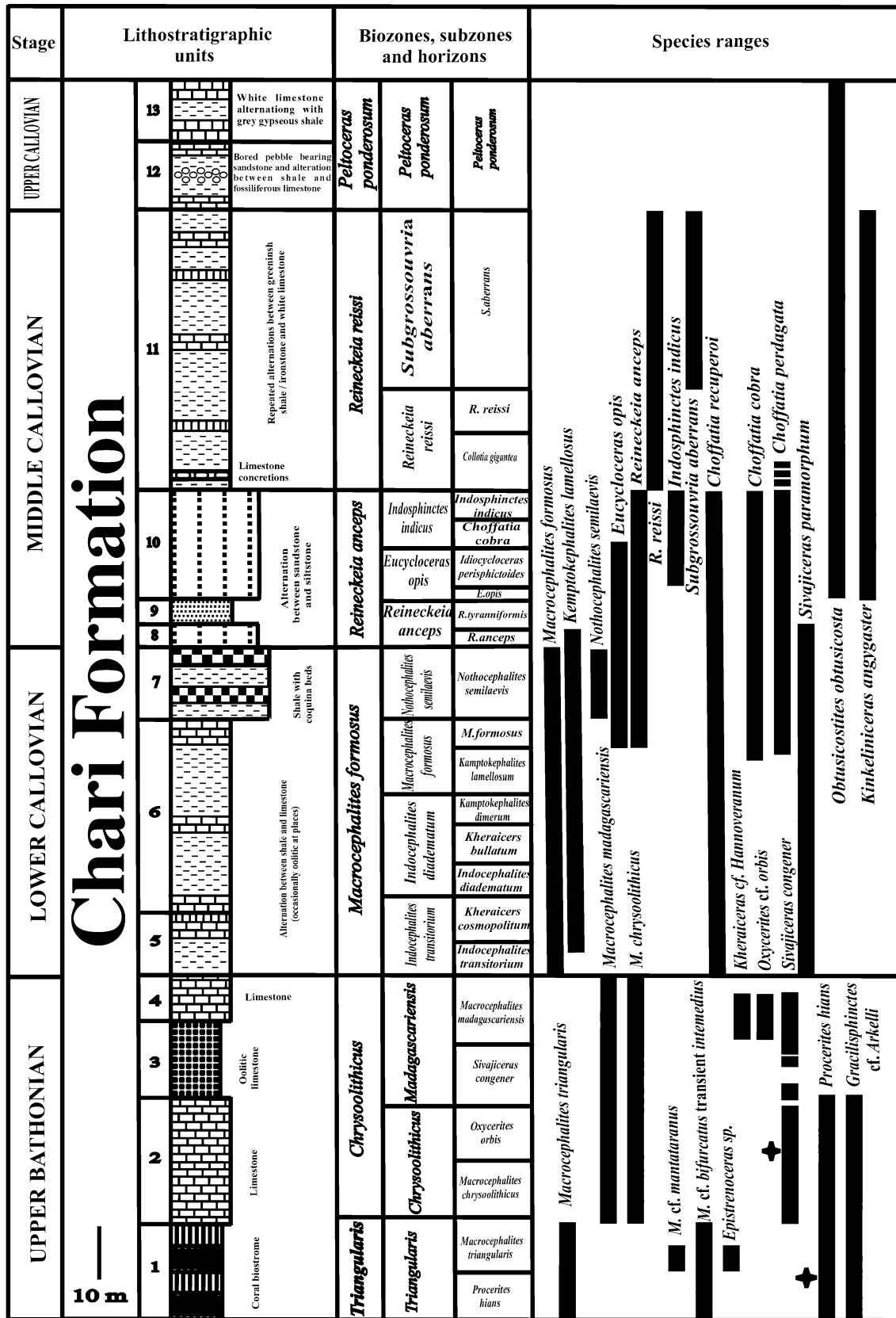


Fig. 2 Stratigraphic column of Jumara section illustrating biostratigraphy and vertical distribution of Sivajiceratinae and other important ammonite taxa. Biozonation is modified after Jana et al. (2000, 2005) and Bardhan et al. (2012). Star indicates the holotype

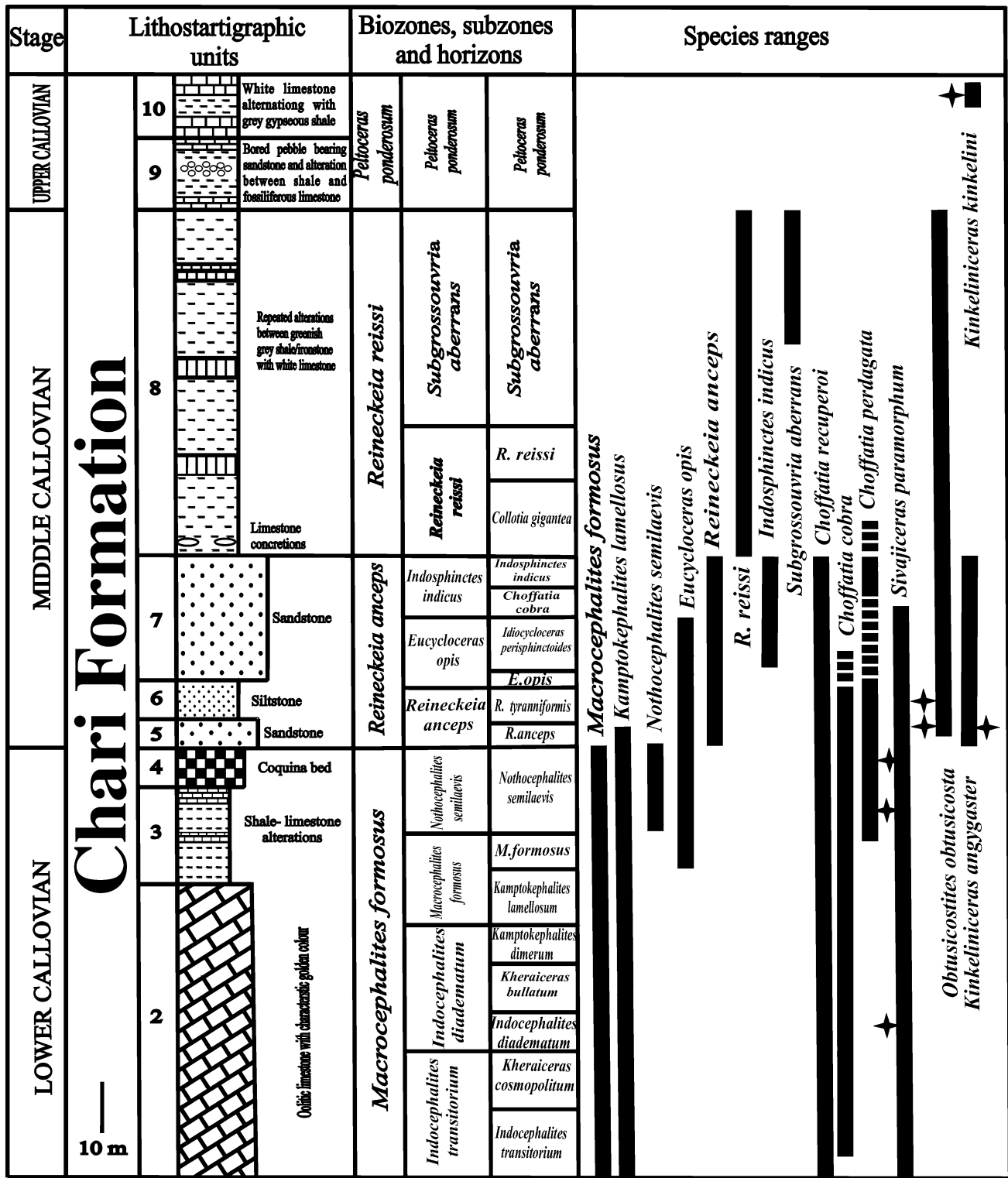


Fig. 3 Stratigraphic column of Keera section illustrating biostratigraphy and vertical distribution of Sivajiceratinae and other important ammonite taxa. Biozonation is modified after Jana et al. (2000, 2005) and Bardhan et al. (2012). Star indicates the holotype

Fig. 4 Distribution of the Sivajiceratinae and the genus *Procerites* is shown against regional biostratigraphic zonation (modified after Jana et al. 2000, 2005; Bardhan et al. 2012)

KUTCH							
		ZONE	SUBZONE	HORIZON	SPECIES RANGE		
CALLOVIAN	UPPER	<i>Peltoceras ponderosum</i>	<i>Peltoceras ponderosum</i>	<i>Peltoceras ponderosum</i>			
						MIDDLE	<i>Reinckeia reissi</i>
	<i>Reinckeia reissi</i>	<i>Reinckeia reissi</i>	<i>Reinckeia reissi</i>				
		<i>Collotia gigantea</i>	<i>Collotia gigantea</i>				
	<i>Reinckeia anceps</i>	<i>Indosphinctes indicus</i>	<i>Indosphinctes indicus</i>	<i>Indosphinctes indicus</i>			
			<i>Choffatia cobra</i>	<i>Choffatia cobra</i>			
		<i>Eucycloceras opis</i>	<i>Idiocycloceras perisphinctoides</i>	<i>Idiocycloceras perisphinctoides</i>			
			<i>Eucycloceras opis</i>	<i>Eucycloceras opis</i>			
		<i>Reinckeia anceps</i>	<i>R. tyranniformis</i>	<i>R. tyranniformis</i>			
			<i>Reinckeia anceps</i>	<i>Reinckeia anceps</i>			
	LOWER	<i>Macrocephalites formosus</i>	<i>Nothocephalites semilaevis</i>	<i>Nothocephalites semilaevis</i>			<i>Nothocephalites semilaevis</i>
				<i>M. formosus</i>			<i>M. formosus</i>
			<i>Macrocephalites formosus</i>	<i>Kamptokephalites lamellosum</i>			<i>Kamptokephalites lamellosum</i>
				<i>Kamptokephalites dimerum</i>			<i>Kamptokephalites dimerum</i>
			<i>Indocephalites diadematum</i>	<i>Kheraicereras bullatum</i>			<i>Kheraicereras bullatum</i>
				<i>Indocephalites diadematum</i>			<i>Indocephalites diadematum</i>
				<i>Kheraicereras cosmopolitum</i>			<i>Kheraicereras cosmopolitum</i>
			<i>Indocephalites transitorium</i>	<i>Indocephalites transitorium</i>		<i>Indocephalites transitorium</i>	
<i>Indocephalites transitorium</i>				<i>Indocephalites transitorium</i>			
BATHONIAN			UPPER	<i>M. chrysoolithicus</i>	<i>M. madagascariensis</i>	<i>Macrocephalites madagascariensis</i>	
	<i>Sivajicereras congener</i>	<i>Sivajicereras congener</i>					
	<i>M. chrysoolithicus</i>	<i>Oxycerites orbis</i>		<i>Oxycerites orbis</i>			
		<i>M. chrysoolithicus</i>	<i>M. chrysoolithicus</i>				
	<i>M. triangularis</i>	<i>M. triangularis</i>	<i>M. triangularis</i>	<i>M. triangularis</i>			
			<i>Procerites hians</i>	<i>Procerites hians</i>			

by disappearance of secondaries and smooth venter. Microconchs small, relatively involute. The size ratio of macroconchs and microconchs (M: m) is 5:1.

Species included: *Sivajicereras congener*, *Sivajicereras paramorphum* and *Sivajicereras fissum*.

Stratigraphical and geographical occurrences: Upper Bathonian to Middle Callovian; Kutch, Madagascar, Tanzania, Somalia and Kenya.

Sivajicereras paramorphum (Waagen, 1875) (Figs. 5, 6a, 7a-j, and 8a-l)

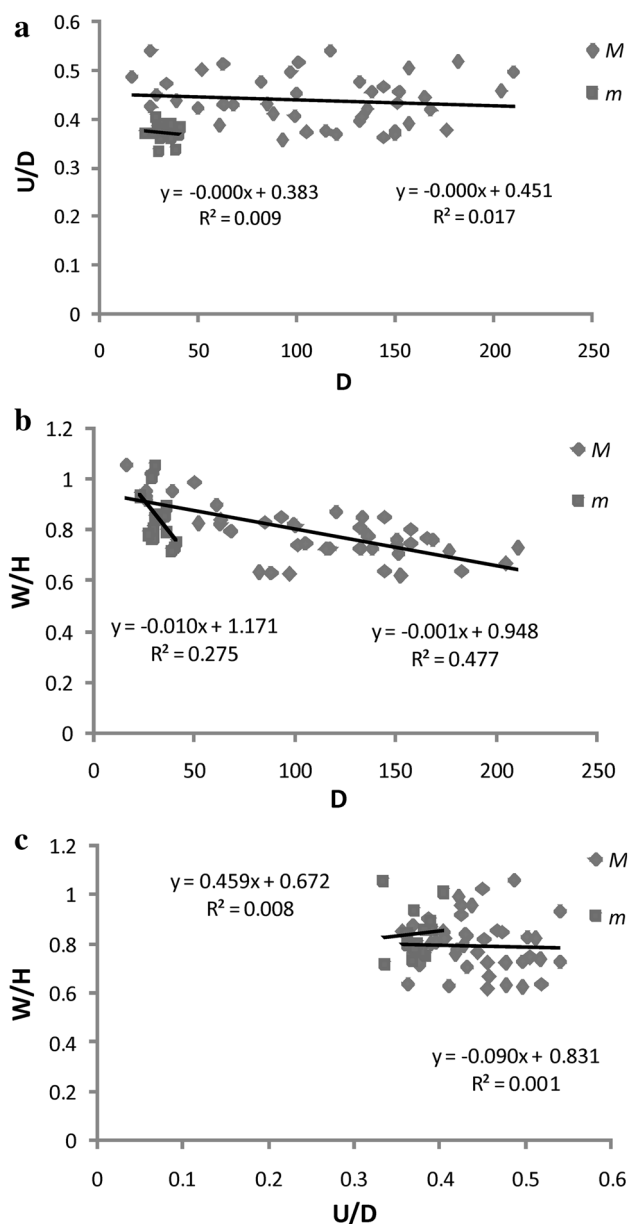


Fig. 5 Bivariate analyses of *Sivajiceras Paramorphum* (Waagen). *M* Macroconch, *m* microconch. **a** Degree of involution versus diameter. **b** Degree of inflation versus diameter. **c** Degree of inflation versus degree of involution

v* 1875. *Perisphinctes paramorphus*, Waagen, p. 162, pl. XLVI, fig. 1 a,b; pl. XLVII, fig. 3 [M]

v 1875. *Perisphinctes* cf. *funatus*, Waagen (non Oppel), p. 155, pl. XLVII, fig. 2 [M]

1921. *Obtusicosites paramorphus* (Waagen); Buckman, p. 42 [M]

1924. *Obtusicosites paramorphus* (Waagen); Spath, p. 13 [M]

1930. *Sivajiceras paramorphum* (Waagen); Spath, p. 35 [M]

1930. *Sivajiceras aureum*, Spath, p. 35 [M]

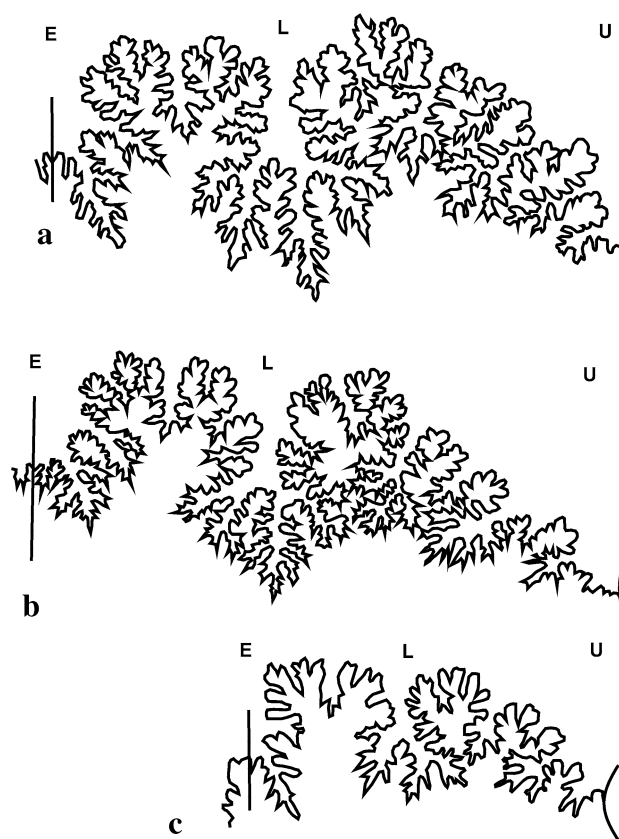


Fig. 6 Septal sutural patterns of three genera. **a** *Sivajiceras paramorphum* (macroconch) at diameter 150 mm, redrawn from Waagen (1875, pl. XLVII, fig. 3); **b** *Obtusicosites obtusica* (macroconch) at diameter 150 mm, redrawn from Waagen (1875, pl. XXXVIII, fig. 2); **c** *Kinkeliniceras angygaster* (macroconch) at diameter 76 mm, redrawn from Spath (1931, pl. LXIII, fig. 2). *E* external lobe, *L* lateral lobe, *U* umbilical lobe. All $\times 1$

v 1931. *Sivajiceras paramorphum* (Waagen); Spath, pl. LXIII, figs. 1 a,b [M]

v 1931. *Sivajiceras kleidos*, Spath, pl. L, fig. 1; pl. LIX, fig. 2 a,b; 3; 9 a,b; pl. LXV, fig. 1 a,b [M]

v 1931. *Sivajiceras aureum*, Spath, pl. LI, fig. 3; pl. LX, fig. 9 a,b; pl. LXIV, fig. 5 a,b, 6 a,b [M]

v 1931. *Sivajiceras* sp. indet. Spath, pl. LXVI, fig. 1 a,c; pl. LXXIX, fig. 6 [M]

v 1931. *Sivajiceras robustum*, Spath, pl. LXVI, fig. 2 [M]

1958. *Sivajiceras besairiei*, Collignon, pl. XX, fig. 84, 84a [M]

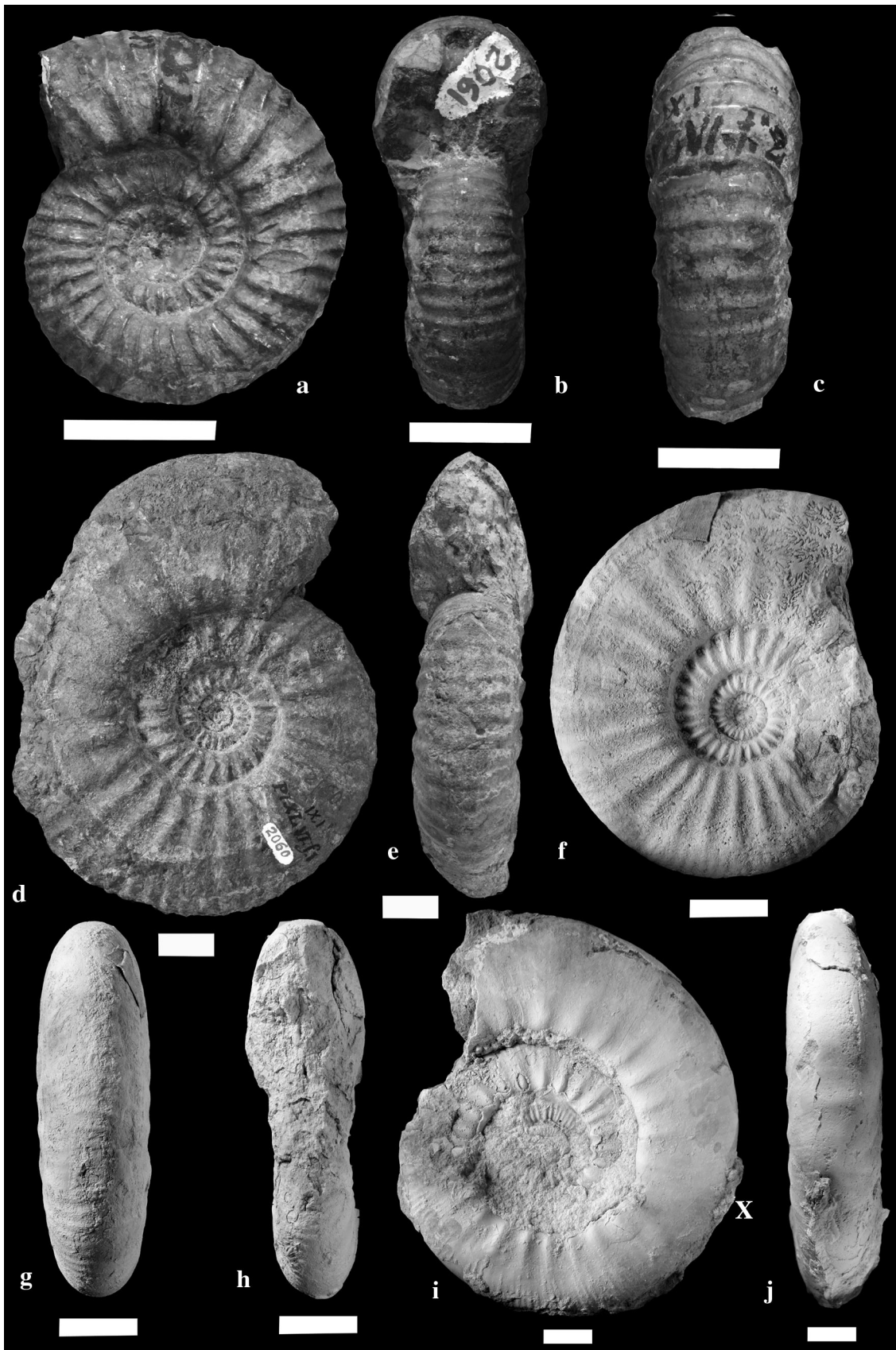
1958. *Kinkeliniceras crassiplanula*, Collignon, pl. XXX, fig. 140 [M]

Holotype: Specimen GSI type no. 2060 [M]

Measurements: See Table 1

Description:

Macroconch: Shell large, maximum adult phragmocone diameter ranges between 144 and 176 mm. At this stage



◀ **Fig. 7** *Sivajiceras paramorphum* (Waagen) [M]. **a–c** A septate young specimen, GSI no. 2061 (Waagen 1875, pl. XLVI, fig. 2a,b); lateral, apertural and ventral views; Golden Oolite of Keera (=Bed no. 2; see Fig. 3). **d, e** Holotype; incompletely preserved adult phragmocone (Waagen 1875, pl. XLVI, fig. 1a,b); GSI type no. 2060; lateral and ventral views; Golden Oolite of Keera (see Fig. 3). **f–h** Topotype; adult phragmocone; Jadavpur University type no. JUM/SP/4; lateral, ventral and apertural views; Golden Oolite of Keera (see Fig. 3). **i, j** Adult specimen with partly preserved body chamber; note disappearance of secondary ribs on body whorl; JUM/SP/2; lateral and ventral views; Bed 7; Jumara (Fig. 2). Scale bar 2 cm. X marks the beginning of body chamber

shell is evolute. Our collection includes two specimens of 204 and 182 mm diameter with incompletely preserved adult body chamber. The larger specimen has adult end-phragmocone diameter of 176 mm and from the trace of umbilical seam, the reconstructed complete diameter appears to be 212 mm. In another specimen, end-phragmocone diameter is 157 mm. Waagen (1875) mentioned but not illustrated a specimen as large as 220 mm in diameter. The species shows wide intraspecific variability with respect to the degree of involution ($U/D = 0.35–0.53$) and inflation ($W/H = 0.6–0.99$), but it is always evolute and compressed (see Fig. 5).

Inner whorls are depressed, widely umbilicate and strongly ornamented. One constriction occurs per half whorl. At 16.5 mm diameter, shell is evolute ($U/D = 0.48$), depressed ($W/H = 1.04$) and has distant primaries ($P = 10$ per half whorl). Spath (1931) also described the inner whorls at 15 mm diameter (Spath 1931, pl. LXI, Fig. 2). However, he did not provide any ventral or apertural views of the specimen. At 29 mm diameter, shell is depressed ($W/H = 1.02$), evolute ($U/D = 0.44$) and has strong, distant primaries ($P = 10$). Both Spath's specimen as well as the present one has the characteristic rursiradiate primaries which bifurcate into secondary ribs ($S = 20$) at or just above the mid-flank. Flank is slightly curved with both umbilical and ventral margins rounded. The venter is broad and round in shape.

At 50 mm diameter, same shell shape and ornamentation continues. Ribs are slightly rursiradiate to rectiradiate and dichotomous (Waagen 1875, pl. XLVI, reproduced here as Fig. 7a–c). Shell is evolute and slightly compressed ($U/D = 0.42$; $W/H = 0.99$). Primary ribs are strong and more ($P = 13$). The early rursiradiate nature of ribbing disappears, giving way to prorsiradiate bifurcating ribs ($S = 26$) which split at or above the mid-flank.

At 105 mm diameter, the shell is still evolute ($U/D = 0.37$) and more compressed ($W/H = 0.74$) than in the earlier preceding whorls. The primaries are strong, thickened and prorsiradiate. They split at or above the mid-flank to produce secondaries which are bi- or trifurcating ($P = 14$ and $S = 36$). Primaries may form bullae near the umbilical edge at the later part. Some variants have only bifurcating

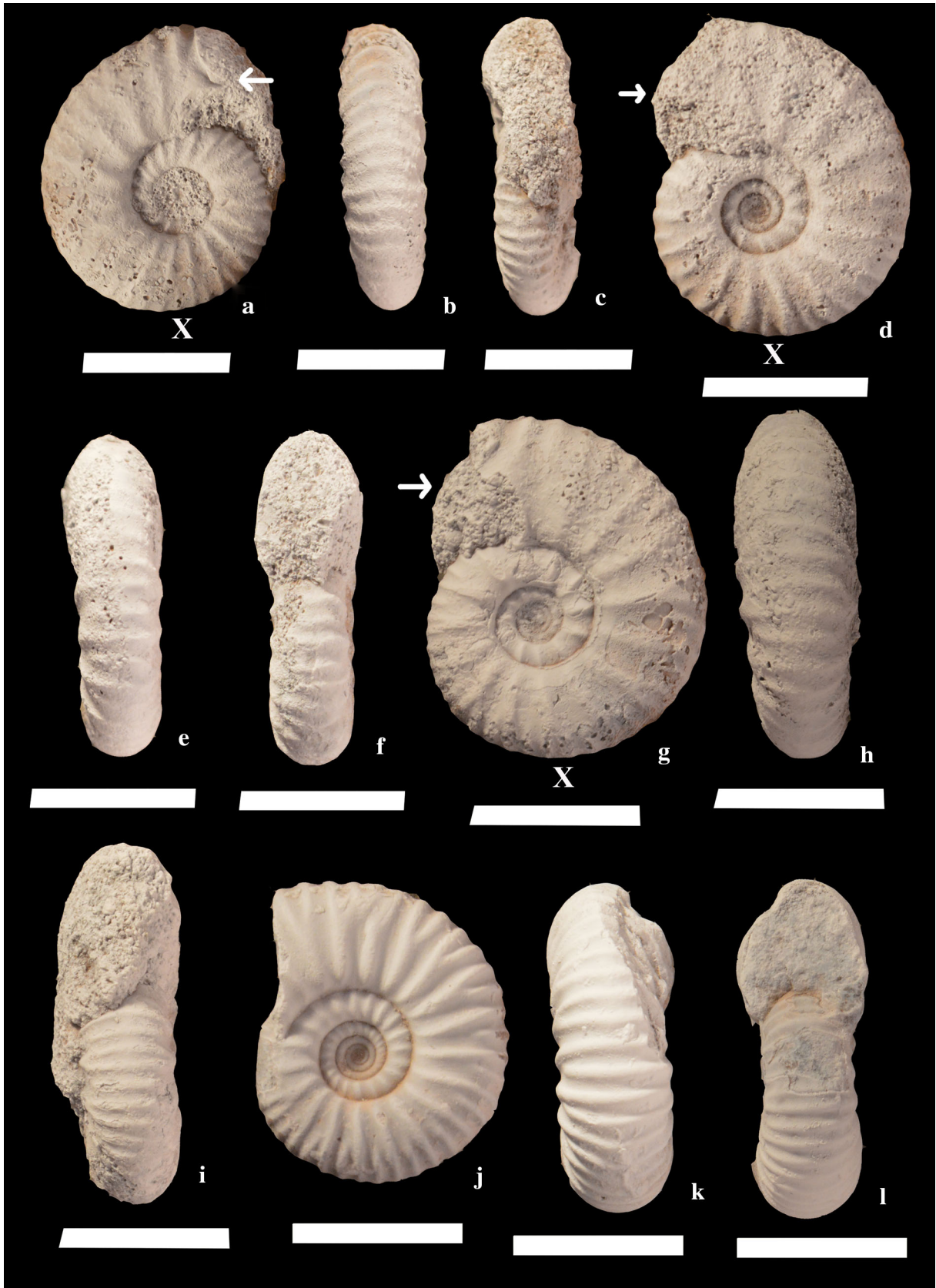
ribs. One constriction per half whorl still present and solitary ribs may occur occasionally and irregularly.

In the adult phragmocone (diameter ranging between 144 and 176 mm), the whorls are evolute (U/D ranges from 0.36 to 0.5 mm), compressed (W/H ranges from 0.6 to 0.8) and distinctly flat. Umbilicus is wide, shallow with gently sloping wall and a gradual umbilical margin. Primaries are strong, thickened, bullae-like and split at or above the mid-flank into two to three secondaries with many short intercalatories. Secondaries show strongly aboral projection. Strength of ribbing in both primaries and secondaries grow unabated up to the end of the phragmocone (Waagen's holotype is highly misleading in this regard, see also Spath's comment, 1931, p. 288). After the adult phragmocone stage (Waagen 1875, pl. XLVI, fig. 1, reproduced here as Fig. 7d, e) secondaries tend to be faint. At the middle part of the whorl, the ribs are somewhat blunt and the connection between the primary and secondary ribs becomes indistinct.

The shell is more evolute in the adult body chamber which occupies 5/6th of the entire outer whorl (Fig. 7i, j). Umbilicus is still wide and shallow ($D = 182$ mm, $U/D = 0.51$) with a gently sloping wall and a gradational margin. The beginning of the body chamber is marked by the disappearance of the secondary ribs and the upper part of the primaries. Flank is flattish and venter is narrow. Strength of primaries becomes weak, but continues up to the preserved end. The bullae at the umbilical margin resemble blunt tubercles which continue up to the preserved body chamber only with a slight loss of strength.

In the present collection, septal sutures are either not well discernible or incomplete. Waagen (1875), however, vividly described the suture line from a topotype (pl. XLVII, fig. 3 and reproduced here in Fig. 6a). Spath (1931) also described the suture lines of his many species of *Sivajiceras*. A complete suture line of Spath's *Sivajiceras* aff. *kleidos* (synonymised here) shows strong resemblance with that of Waagen's (1875) specimen: First lateral lobe long with five branches; external saddle broad with a well-developed secondary lobe; second lateral lobe narrow terminating in two small branches and shorter than first lateral lobe; first lateral saddle also narrow with two secondary small lobes; auxiliary lobes are hanging and form a large sutural lobe which is shorter than first lateral lobe.

Microconch: The adult shell is flat to slightly rounded, compressed and resembles the inner whorls of the macroconch (compare Waagen 1875, pl. XLVI, fig. 2 which is reproduced here in Fig. 7a–c with the present adult microconch in Fig. 8a–c). Inner whorls have strong and distant primaries ($P = 6–7$). Umbilicus is shallow to slightly crateriform with gradual margin and sloping wall. Adult phragmocone diameter ranges from 30 to 36 mm and



◀ **Fig. 8** *Sivajiceras paramorphum* (Waagen) [m]. **a–c** Allotype with preserved lappet; note narrow, short lappet preceded by the deep terminal constriction; JUM/SP/22; lateral, ventral and apertural views; Golden Oolite of Keera (see Fig. 3). **d–f** Adult with trace of a broken lappet; JUM/SP/23; lateral, ventral and apertural views; Golden Oolite of Keera. **g–i** Adult with trace of a broken lappet; JUM/SP/21; lateral, ventral and apertural views; Golden Oolite of Keera (see Fig. 3). **j–l** Adult phragmocone; JUM/SP/26; lateral, ventral and apertural views; Bed 6; Jumara (see Fig. 2). Scale bar 2 cm. Arrows indicate the lappet. X marks the beginning of body chamber

is evolute as well as compressed ($U/D = 0.35$ to 0.38 , $W/H = 0.76$ to 0.84). Adult body chamber occupies more than half of the outer whorl. Ribs on outer shell are bifurcating with irregularly placed solitaries. Furcation takes place at or above the mid-whorl. Both primaries and secondaries continue with no loss of strength up to the peristome. Ribs are mostly rectiradiate and secondaries cross the venter with slight forward projection. Narrow, short lappet preceded by deep terminal constriction present.

Remarks: Spath (1931) described as many as eight species of *Sivajiceras* from the Lower Callovian of Kutch. He himself admitted that these species were interconnected by numerous transitional forms (Spath 1931, pp. 283–293). Spath's species were mostly macroconchs and most of them lacked the body chamber. We here clubbed most of them into the present species *Sivajiceras paramorphum*. They show considerable similarities and form a spectrum of continuous intraspecific variability. However, we consider *S. fissum* as a distinct species (see below).

Sivajiceras paramorphum has a microconch with a smaller diameter (maximum 40 mm) and a less evolute shell compared to the microconch of the older *Sivajiceras congener*. However, the degree of inflation is similar to that of *S. congener*. *S. congener* has more number of primary and secondary ribs ($P = 12$, $S = 38$) than the present species. Even in inner whorls, primaries are numerous in the microconch of *S. congener* ($P = 17$) than in the present microconch ($P = 6–7$). Ribs of *S. congener* become stronger and slightly flexuous near the peristome (Callomon 1993, pl. 24, fig. 2 a,b) while these features are not noted in the present microconchiate form. Both species also differ in the length of the adult body chamber. In *S. congener*, the entire outer whorl is occupied by the body chamber while in *S. paramorphum*, the body chamber length slightly exceeds half of the adult outer whorl. However, both these two microconchs have a similar pattern of ribbing that primaries are mostly bifurcating with occasional solitaries.

While describing his *Perisphinctes paramorphus*, Waagen (1875) mentioned that the adult outer whorl is entirely smooth. We here describe one specimen with most of the parts of the adult body chamber preserved. It shows that while primary ribs with attenuating strength continue at least up to the preserved end, the secondaries become

obsolete from the beginning of the body chamber and finally disappear.

The present macroconch of *S. paramorphum* shows a strong resemblance with that of *S. congener* from the Upper Bathonian beds of the same section at Jumara. Resemblance, however, is restricted to the phragmocone for which they are virtually indistinguishable in terms of degree of involution and inflation (see for comparison Callomon 1993, pl. 23 and Roy et al. 2007, fig. 6. 9–10). The only differences, albeit subtle, are found in the number of primary and secondary ribs. In the younger *S. paramorphum*, primaries are more (average 16 per half whorl) while in *S. congener*, they are less (average 11–12 per half whorl). There are three to four secondaries (see also Callomon 1993) in the young stage of *S. congener*, while in *S. paramorphum*, the number of secondaries decreases to two to three.

However, the most diagnostic difference found comes in the nature of dimorphism. The present microconch is very small (about 40 mm in adult diameter) and the dimorphic size ratio (M: m) is 5:1, while in *S. congener* the ratio is M: m = 3: 1. Callomon (1993, pl. 24) described a nearly complete microconch of *S. congener* which has two to three secondaries on the body whorl, but in the present microconch, the primaries are characteristically bifurcating.

Sivajiceras besairiei described by Collignon (1958, pl. XX, fig. 84, 84a) from the Lower Callovian of Madagascar is a large species with a preserved shell diameter of 310 mm. It strongly resembles the present species in degree of involution and inflation. The body chamber appears to be partially preserved in the Madagascan species and a similarity is marked by weak primaries and the disappearance of secondaries. However, the phragmocone has flexuous and more primary ribs ($P = 18$ at middle whorl). In the present species instead, ribs are mostly rectiradiate and distantly spaced (at similar whorl diameter, $P = 14$).

Sivajiceras fissum (J. de C. Sowerby, 1840) (Fig. 9a–d)

v* 1931. *Sivajiceras fissum*, Spath, pl. LVI, fig. 6a–c [M]
v 1931. *Sivajiceras subfissum*, Spath, pl. LVI, fig. 3a–c [M]

Holotype: Specimen NHMUK C25433[M]

Measurements: see Table 1.

Remarks: Spath (1931) described this species on the basis of a poorly preserved holotype. According to him, the species has “extremely coarse and blunt ribbing across the siphonal area of the body chamber” (p. 294). *Sivajiceras paramorphum* differs from the present species ($D = 78$ mm) in having a larger phragmocone and a coarser ribbing. Adult ribs in *S. fissum* have 2–3 secondaries, and therefore, cannot be considered as microconchiate form. Moreover, the species is restricted only to a Lower Callovian horizon (Spath's ‘*rehmanni* zone’). We

Table 1 Measurements of all macroconchs and microconchs of *Sivajiceras paramorphum* and *S. fissum*

Specimen no	Description	D	U	W	H	P	S	RW	RS	U/D	W/H
<i>Sivajiceras paramorphum</i>											
JUM/K/SP/1[M]	Body chamber	204	93	46	69					0.45	0.66
	Phragmocone	176	66	40	56					0.37	0.71
JUM/J/SP/2[M]	Body chamber	182	94	38	60					0.51	0.63
	End-phragmocone	157	79	38	51	14		6.44	5.3	0.5	0.74
JUM/K/SP/3[M]	Phragmocone	144	52	35	55	15		5.42	4.7	0.36	0.63
JUM/K/SP/4[M]	Phragmocone	150	56	42	57	15		5.55	4.87	0.37	0.73
JUM/J/SP/5[M]	Phragmocone	152	69	37	60	13		6.57	6.13	0.45	0.61
	Inner whorl	68	29	27	34					0.42	0.79
JUM/K/SP/6[M]	Phragmocone	151	65	38	54	16		4.17	3.54	0.43	0.7
JUM/J/SP/7[M]	Phragmocone	144	67	40	47	18		4.84	4.23	0.46	0.85
JUM/J/SP/8[M]	Phragmocone	117	63	29	40	14		5.53	4.9	0.53	0.72
JUM/K/SP/9[M]	Phragmocone	97	48	20	32	18		3.8	3.9	0.49	0.62
JUM/J/SP/10[M]	Phragmocone	82	39	12	19					0.47	0.63
JUM/K/SP/11[M]	Phragmocone	88	36	22	35	17		2.5	2.84	0.4	0.62
JUM/J/SP/12[M]	Phragmocone	101	52	31	42	12		3.4	3.3	0.51	0.73
	Inner whorl	52	26	19	23					0.5	0.82
	Inner whorl	26	14	11	11.8					0.53	0.93
JUM/J/SP/13[M]	Inner whorl	26	11	11	12			1.66	1.71	0.42	0.91
JUM/U/SP/14[M]	Phragmocone	157	61	44	55	14		5	7	0.38	0.8
	Phragmocone	132	52	39.5	49	13	39	5	7	0.39	0.8
JUM/K/SP/15[M]	Phragmocone	85	36.5	27	32.5	14		4	4.9	0.42	0.83
JUM/K/SP/16[M]	Phragmocone	132	62.7	40.5	56					0.47	0.72
	Inner whorl	62.7	32	25	30.4					0.51	0.82
JUM/K/SP/17[M]	Phragmocone	138	62.6	40.5	56					0.45	0.72
	Inner whorl	63	27	26	31					0.42	0.83
JUM/J/SP/18[M]	Inner whorl	26	11	10.5	11	12	24	1.15	1.32	0.42	0.95
JUM/U/SP/19[M]	Inner whorl	34	16	11	13	11	23	1.28	1.52	0.47	0.84
JUM/J/SP/20[M]	Inner whorl	29	13	13.3	13			1	1.7	0.44	1.02
	Inner whorl	16.5	8	7.4	7	10		0.67	0.49	0.48	1.05
GSI 2064[M]	Adult phragmocone	105	39	32	43	15	34	3.12	4.26	0.37	0.744
	Phragmocone	93	33	31	36.5	15	37	3	4.12	0.35	0.84
GSI 2060[M] ^a	Holotype, adult phragmocone	150	55	41.5	54.5	14		4.45	5.16	0.36	0.76
	phragmocone	115	43	34	47	14	30	4	5	0.37	0.72
GSI 2065[M]	Adult phragmocone	168	70	44	58	16	49	4.5	5.5	0.41	0.75
	Phragmocone	133	53.5	42	49.5					0.4	0.84
	Inner whorl	99	40	30	36.5	15		3.63	4.5	0.4	0.82
GSI 2061[M]	Phragmocone	50	21	20.2	20.4	15	23	2.26	3.05	0.42	0.99
	Inner whorl	39	17	15	15.7	16	26	1.6	2.28	0.43	0.95
GSI 16069[M]	Phragmocone	210	104	48.6	66.75			6.5	7.8	0.49	0.72
	Phragmocone	165	73	39	51	19		4.5	5.9	0.44	0.76
	Inner whorl	136	57	38	49	19		4	5.2	0.41	0.77
GSI 16072[M]	Phragmocone	100	45	31	38	9	19	3.5	5	0.45	0.81
GSI 16070[M]	Phragmocone	120	44	41	47	12	38	4.21	3.5	0.36	0.87
	Inner whorl	61	23.5	22.5	25	7		3	3.5	0.38	0.9
JUM/J/SP/21[m]	Body chamber	40.55	15.5	12.6	16.7	7	19	2.2	2.7	0.38	0.75
	Phragmocone	30.5	11	11	13	9	22	2	2.55	0.36	0.84
JUM/J/SP/22[m] ^a	Allotype, body chamber	40	14.7	11	15	9	20	1.75	2.62	0.36	0.73
	Phragmocone	32	12.5	11.5	13.4	10	20	1.66	2.55	0.38	0.85

Table 1 continued

Specimen no	Description	D	U	W	H	P	S	RW	RS	UID	WH
JUM/J/SP/23[m]	Body chamber	38.36	12.9	11.7	16.26	9	20	1.86	3	0.33	0.71
	Phragmocone	29	11	9.48	12.32	9	17	1.6	2.32	0.37	0.76
JUM/J/SP/24[m]	Phragmocone	36	13	11.5	14.5	10	21	2.04	2.6	0.36	0.79
	Inner whorl	29.5	11	9.84	12.25	11	22	1.62	1.87	0.37	0.8
JUM/J/SP/25[m]	Phragmocone	35	13.4	12	14	8		1.82	2.35	0.38	0.85
	Inner whorl	27	10	9	11.5	9	20	1.7	2	0.37	0.78
JUM/J/SP/26[m]	Phragmocone	36	14	13.4	15	11	21	1.72	1.94	0.38	0.89
	Inner whorl	28.5	11.5	12	11.9	11	22	1.62	1.81	0.4	1
JUM/J/SP/27[m]	Phragmocone	30	10	14	13.3	8	18	1.86	2.34	0.33	1.05
	Inner whorl	23	8.5	9.86	10.56	9		1.52	1.84	0.36	0.93
<i>Sivajiceras fissum</i>											
NHMUK C 25433 ^a	Holotype, body chamber	100	39	36	36	13	29			0.39	1
NHMUK C 51958	Phragmocone	83	36.5	32	32	13				0.44	1

^a The holotype/allotype

provisionally assigned it as a distinct species and considered it as an evolutionary offshoot with a very short temporal range.

Genus *Obtusicostites* Buckman, 1921

Type species: *Perisphinctes obtusicosta* (Waagen, 1875)

Diagnosis: Macroconch large (maximum $D = 165$ mm), evolute ($UID = 0.3-0.38$). Phragmocone with bullae-like primary ribs, body chamber thoroughly ribbed with no sign of attenuation of strength at least up to the preserved end. Microconch strongly ribbed. The size ratio of macroconchs and microconchs (M:m) is 3:1.

Species included: *Obtusicostites obtusicosta* and *Obtusicostites devi*.

Stratigraphical and geographical occurrences: Middle to Upper Callovian; Kutch, Madagascar and Tanzania.

Obtusicostites obtusicosta (Waagen, 1875) (Figs. 6b, 10, 11a–m, and 12a–l)

v* 1875. *Perisphinctes obtusicosta*, Waagen, p. 146, parts, pl. XXXVIII, fig. 1a,b; p. 146, pl. XXXVIII, fig. 2; p. 146, pl. XXXVIII, fig. 3 a,b [M]

v 1875. *Perisphinctes dhosaensis*, Waagen, p. 149, pl. XXXVIII, fig. 4a–c [m]

v 1875. *Perisphinctes omphalodes*, Waagen, p. 150, pl. XXXVIII, fig. 2a,b [m]

v 1931. *Obtusicostites obtusicosta* (Waagen); Spath, pl. LV, fig. 2; pl. LXIV, fig. 3 a,b [M]

v 1931. *Obtusicostites waageni*, Spath, pl. LIII, fig. 2a,b; pl. LXXX, fig. 1 a,b [m].

v 1931. *Obtusicostites buckmani*, Spath, pl. XLIX, fig. 9; pl. LIII, fig. 3a,b; pl. LXII, fig. 8 [M]

v 1931. *Obtusicostites devi*, Spath, parts, pl. XLV, fig. 5; pl. LII, fig. 2a,b; pl. LXV, fig. 3 [M]

v 1931. *Obtusicostites devi*, Spath, parts, pl. LV, fig. 4 [M]

v 1931. *Obtusicostites ushas*, Spath, pl. LII, fig. 6; pl. LIII, fig. 1 a,b; pl. LVI, fig. 1; pl. LVII, fig. 3; pl. LXIII, fig. 6 [M]

v 1931. *Kinkeliniceras crassiplanula*, Spath, pl. LVIII, fig. 4, 5; pl. LXV, fig. 4 a,b [M]

v 1931. *Obtusicostites* aff. *ushas*, Spath pl. LVII, figs. 7a,b [m]

v 1931. *Hubertoceras dhosaense*, (Waagen); Spath, pl. LXXIV, figs. L a,b [m].

v 1931. *Hubertoceras hubertus*, Spath, parts, pl. LVII, fig. 4a–c; pl. LIX, fig. 1 [m]

v 1931. *Hubertoceras omphalodes*, (Waagen), Spath, pl. XLIX, figs. 7 a,b; pl. LXI, fig. 4; pl. LXV, fig. 2; pl. LXVII, fig. 9 [m]

1958. *Obtusicostites* aff. *obtusica*, (Waagen); Collignon, pl. XXIX, fig. 133 [M]

1958. *Obtusicostites ushas*, (Spath), Collignon, pl. XXIX, fig. 131 [M]

1958. *Obtusicostites buckmani*, (Spath), Collignon, pl. XXXI, fig. 143 [M]

1958. *Obtusicostites devi*, (Spath), Collignon, pl. XXXI, fig. 144 [M]

1958. *Kinkeliniceras kinkelini*, (Dacque), Collignon, pl. XXIX, fig. 135 [m]

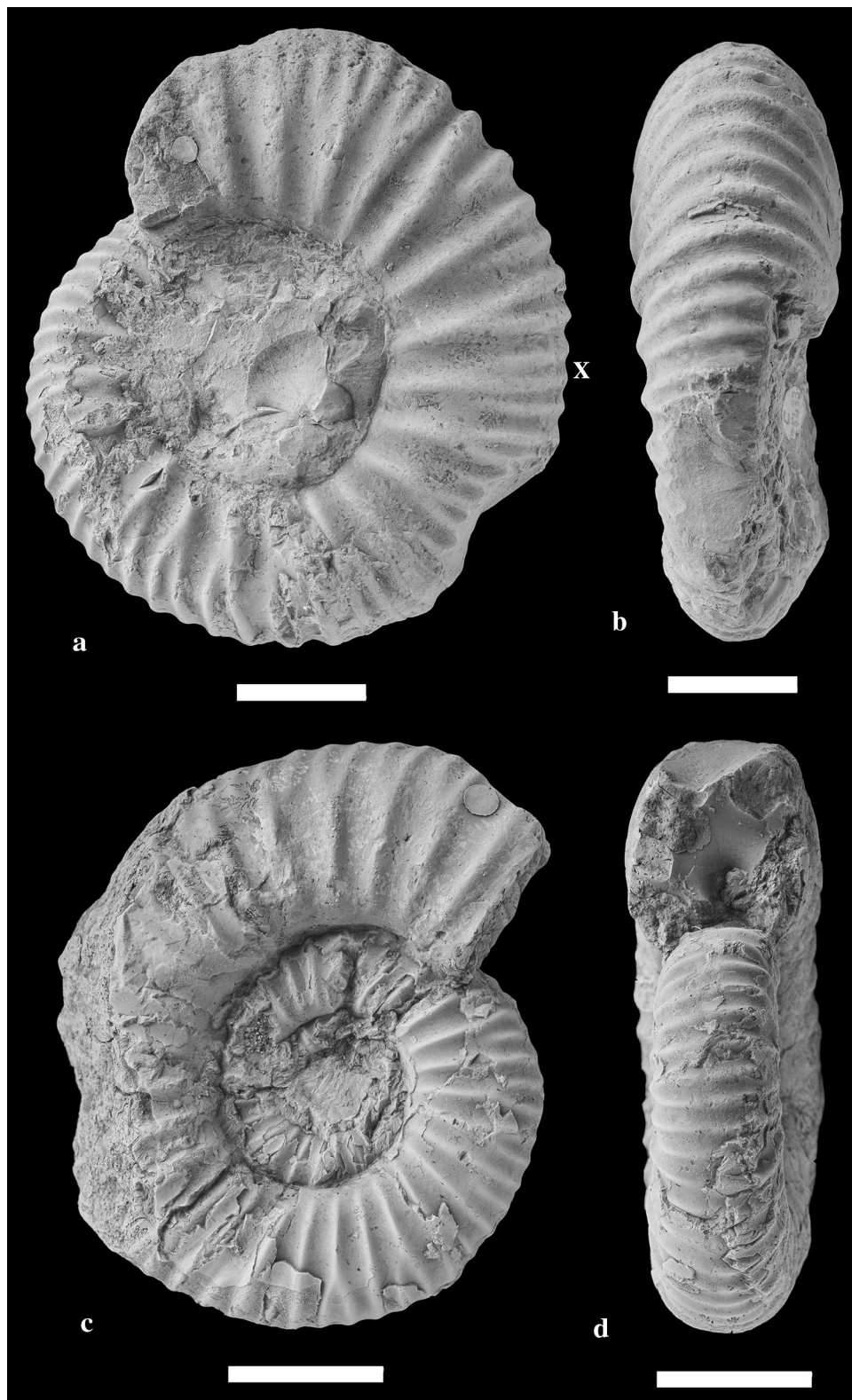
Holotype: Specimen GSI type no. 2032[M]

Measurements: see Table 2.

Description:

Macroconch: Like *Sivajiceras*, this species also exhibits great ontogenetic changes in degree of involution and

Fig. 9 *Sivajiceras fissum* (Sowerby) [M]. **a, b** Holotype; adult phragmocone; note very coarse and blunt ribbing; (Spath 1931, pl. LVI, fig. 6a,c; now archived in Natural History Museum, U.K., no. C 25433); lateral and ventral views; 'Rehmanni zone' (=Bed no. 7, Jumara, see fig. 2). **c, d** Holotype; adult phragmocone (Spath 1931, pl. LVI, fig. 3a,c, Natural History Museum, U.K., no. C 51958); lateral and apertural views; 'Rehmanni zone of Lower Callovian of Badi'. Scale bar 2 cm



inflation (Fig. 5). At diameters below 50 mm, the shell is evolute ($U/D = 0.3\text{--}0.38$) and depressed ($W/H = 1\text{--}1.09$). Primary ribs at this stage are very strong, fewer and distant

($P = 6\text{--}7$). Flanks are slightly curved with a steep umbilical wall and distinct margin. Primary ribs originate from the umbilical wall and rectiradial.

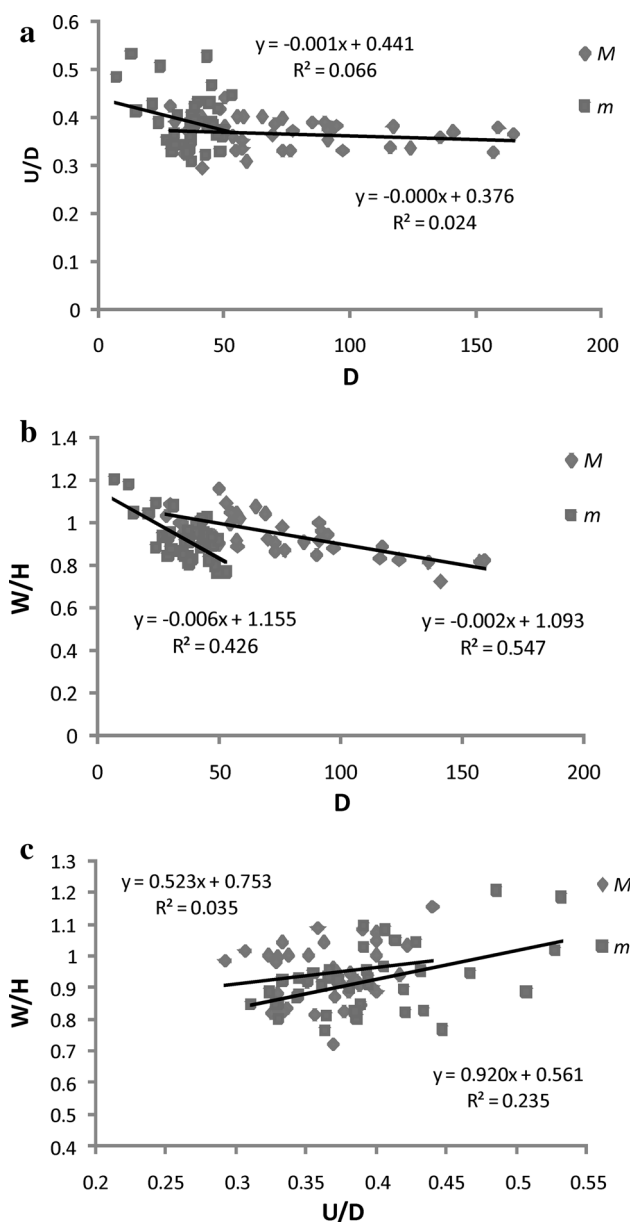


Fig. 10 Bivariate analyses of *Obtusicostites obtusicosta* (Waagen). *M* Macroconch, *m* Microconch. **a** Degree of involution versus diameter. **b** Degree of inflation versus diameter. **c** Degree of inflation versus degree of involution

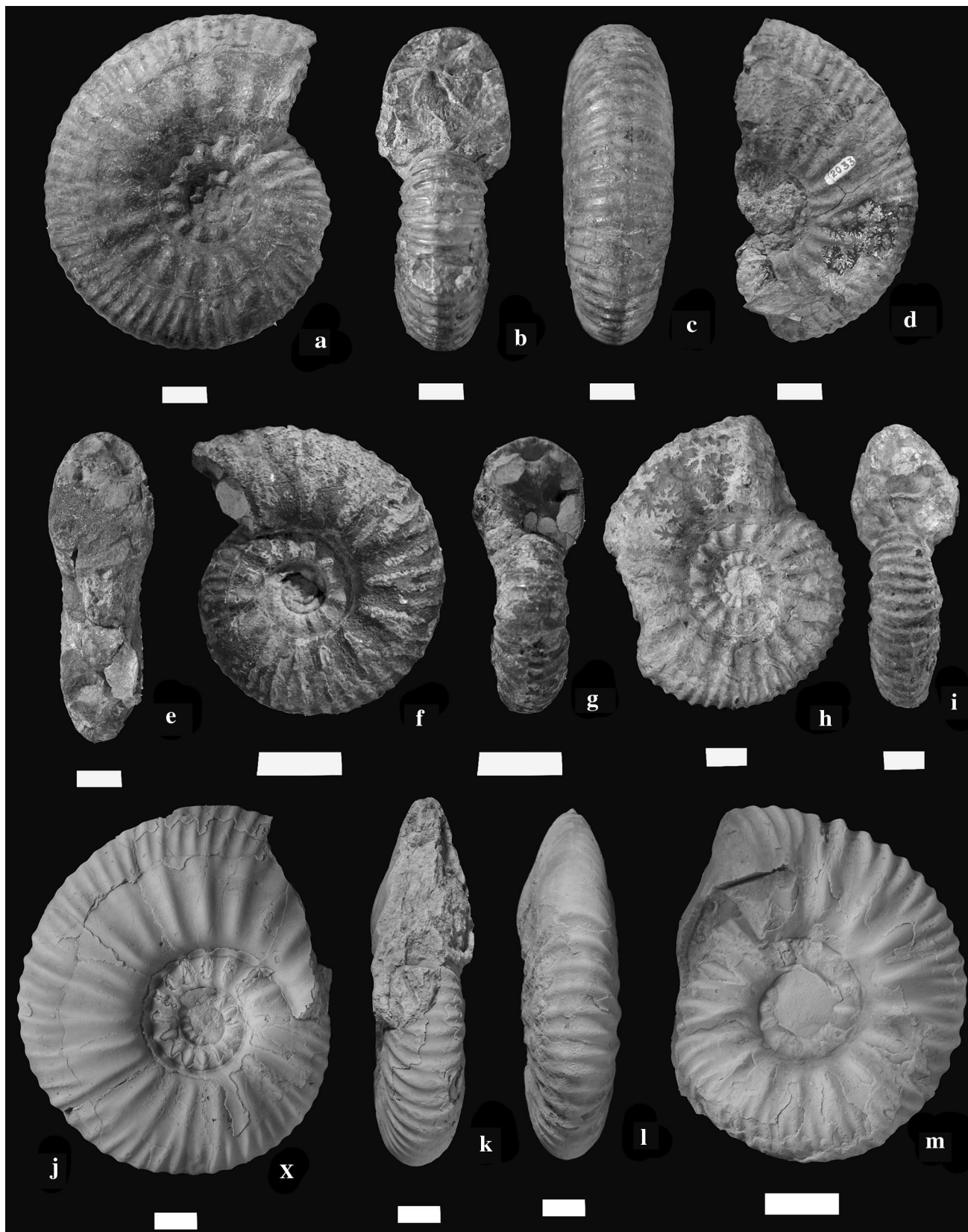
Shells are more or less squarish and evolute up to the middle whorls of the phragmocone ($D = 57\text{--}115$ mm, $U/D = 0.3\text{--}0.39$, $W/H = 0.8\text{--}1$). Primary ribs are still sparse ($P = 7\text{--}9$). Primaries split into two–three secondaries which pass more or less straight across over the venter. Venter is narrow. Solitary ribs of varying length are also present and irregularly placed. The point of furcation is below the mid-whorl and the junction between primary and secondary ribs become indistinct on shell, but are distinct on the internal mould. Primaries are low, broad and may form bullae. Umbilical wall is distinctly sloping with gradual margin.

The end of the adult phragmocone may be marked by a shallow and broad constriction. Diameter at this point ranges from 124 to 159 mm. The holotype (Waagen 1875, pl. XXXVIII, fig. 1a-b) which is reproduced here (Fig. 11a–c) represents the end-phragmocone stage and the whole outer whorl is missing as evident from the trace of the umbilical seam. At the adult end-phragmocone stage, the shell becomes more compressed ($W/H = 0.75\text{--}0.81$) and relatively involute ($U/D = 0.32\text{--}0.38$). Flanks are flattish with strong primary and secondary ribs. Umbilicus has sloping wall and gradual margin. The numbers of primary and secondary ribs vary considerably during ontogeny. They increase from P (7–9) and S (30–33) in the inner whorls to P (9–11) and S (33–36) in the adult phragmocone. Waagen's (1875) restored painting diagram of the holotype showing 61 secondaries is incorrect. The number of primaries increases further in the adult body whorl. Secondaries show mainly trifurcation and occasional solitaries in the adult phragmocone stage. The illustration of the holotype by Waagen (1875) is highly restored in this regard and shows incorrectly four to five secondaries originating from the bullae-like primaries which were located near the umbilical edge, but actually the trifurcation takes place at or near the mid-flank (Fig. 11a–c).

The adult body chamber is preserved in one of our specimens where it occupies more than half of the outer whorl and is thoroughly and relatively densely ribbed (Fig. 11j–l). At about 165 mm diameter, primary and secondary ribs are 13 and 32, respectively. Ribs continue and show no sign of attenuation at least up to the preserved end. There is a change in the ribbing pattern. Ribs are dominantly bifurcating while it was also trifurcating in the phragmocone stage. Moreover, length of primaries increases in the body chamber, in the latter part of the body chamber, the primary ribs furcate higher on the flank. This feature indicates that the body chamber is adult. The adult body whorl is compressed ($W/H = 0.7$) with a wider flank and a narrow venter and the shell is relatively less evolute ($U/D = 0.33$). Our specimen is however slightly crushed near the end. Primaries are slightly curved prorsiradiately and secondaries, which originate at the mid-whorl, projects further forward while passing the very narrow venter.

Spath (1931) mentioned that larger *Obtusicostites obtusicosta* may be entirely smooth like *Sivajicerias* or *Procerites* but he did not illustrate any specimen. We believe that *Obtusicostites* is ribbed to the end and thus retains neotenusly the phragmocone stage of *Sivajicerias* up its adulthood.

Septal sutures of this species were well studied by both Waagen (1875) and Spath (1931). Waagen (1975) described and illustrated the external suture from a topotype (pl. XXXVIII, fig. 2, here refigured as Fig. 6b), while Spath



◀ **Fig. 11** *Obtusicoelites obtusicoelata* (Waagen) [M]. **a–c** Holotype; adult phragmocone; GSI no. 2032 (Waagen 1875, pl. XXXVIII, fig. 1a,b); lateral, apertural and ventral views; from ‘*Perisphinctes anceps*’ beds of Keera (=Bed nos. 5–7, see Fig. 3). **d, e** Incompletely preserved adult body chamber; GSI no. 2033 (Spath 1931, pl. LIII, fig. 2a,b); lateral and apertural views; from ‘*Perisphinctes anceps* beds’ of Keera. **f, g** Young specimen; note bullae-like primary ribs; GSI no. 2034 (Waagen 1875, pl. XXXVIII, fig. 3a,b); lateral and apertural views; ‘*athleta* beds’ of North Gudjinsir. **h, i** Adult phragmocone; GSI no. 16077 (Spath 1931, pl. LV, fig. 4); lateral and apertural views; from ‘*athleta* beds’ of Fakirwadi (=Bed nos. 12–13, Jumara, see fig. 2). **j–l** Adult with preserved body chamber; JUM/OO/1; lateral, apertural and ventral views; Bed 11; Jumara. (M) Phragmocone; JUM/OO/4; lateral view; Bed 11; Jumara. *Scale bar* 2 cm. *X* marks the beginning of body chamber

(1931) described the external suture from the holotype (pl. LV, Fig. 2). In both cases, sutures were studied at adult phragmocones diameters of nearly 140 mm. Two sutures of the two specimens show considerably intraspecific variability. In the topotype, the external saddle is broad with a deeply incised secondary lobe; first lateral lobe is relatively narrow and longer than the siphonal lobe which has five terminating branches; the first lateral saddle is narrow with a deep asymmetrical lobe. The second lateral lobe is hanging, narrow and short. The second lateral saddle is also short and oblique with a very large secondary lobe. However, in the holotype at about the same diameter, the external saddle is rather narrow. First lateral lobe although longer than the siphonal lobe has only three terminating branches; second lateral lobe as Spath (1931) correctly described ‘become merely an incision in the lateral saddle’.

Microconch: The microconch shows great variation in shell involution ($U/D = 0.33–0.43$), inflation ($W/H = 0.68–1.09$) and ornamental density. Shell is compressed to depressed (Fig. 10). Flanks may be flattish to rounded with perisphinctoid (for more evolute shell) to crateriform (relatively less evolute shell) coiling. Shell is small, maximum diameter of adult shell ranges between 37 and 50 mm. In inner whorls, 7–14.5 mm, shell is more evolute ($U/D = 0.41–0.44$) and depressed ($W/H = 1.05–1.2$). Here, the primaries are strong and widely spaced ($P = 7–8$).

Adult phragmocone has diameter ranges between 25 and 37 mm; shell is still evolute ($U/D = 0.4–0.42$) and depressed ($W/H = 0.95–1.09$). Primaries are variable in number ($P = 8–12$). There are hardly differences in strength between primary and secondary ribs (isocostate). Primaries are distant and into 2–3 secondaries. Primaries are rectiradiate and secondaries may be prorsiradiate and passing over the venter with forward bend. There are occasional solitaries which are relatively fine.

Beginning of the adult body chamber is marked by a sudden change in the strength of ribbing, especially the

primaries (varicostate, see Fig. 12i, j). Primaries at this stage range from 12 to 15 per half whorl. Primaries branch at the mid-flank to higher flank into two secondaries. Some variants become compressed and have flatter whorl sides. Depressed variants have rounded flanks and a wider venter. They are involute and have less ribs ($P = 7–8$; e.g. *H. dhosaensis* variant, see Fig. 13d–f). Umbilical margin is distinct, wall steep to overhanging. Peristome is marked by narrow, deep, long lappet (see Fig. 13k, l) with broad base which is preceded by deep terminal constriction.

Remarks: Spath (1931) described eight species of *Obtusicoelites* in which two species are herein considered unrelated, i.e. *O. nandi* and *O. purpuratus*. The lateral view of a specimen of *O. nandi* illustrated by Spath (pl. LXVII, fig. 2a) is poorly preserved and can be easily discounted from *O. obtusicoelata* by its well-defined straight, multiple dense ribbing. Besides, the ventral view of the holotype of *O. nandi* (pl. LVII, Fig. 5) shows peculiar fine, thread-like ribs along in-between the secondaries. *O. purpuratus* was confused by Spath himself with *Kinkeliniceras*. We therefore excluded these two species from the genus *Obtusicoelites* and at present we cannot assign them to any species of related genera.

We finally described two species of this genus, i.e. *O. obtusicoelata* and *O. devi*. The majority of the species within the genus *Hubertoceras* are now considered as microconchs of *O. obtusicoelata*. However, *Hubertoceras arcicosta* and *H. mutans* were not included. *Hubertoceras?* sp. nov. and *O. aff. ushas* as described by Spath (1931) are considered as the macroconchs of *O. devi*. Spath’s *Hubertoceras hubertus* displays extreme variability and we included some of the variants as microconchs of the present species. The two other variants (*H. hubertus* var. *densicostata* and *H. hubertus* var. *rotunda*) are now designated as microconchs of *O. devi*.

Hubertoceras ranaivoi (Collignon 1958, pl. XXIX, fig. 129) is more evolute and larger than the present microconch. *Obtusicoelites ankoboensis* (Collignon 1958, pl. XXIX, fig. 132) is distinguished from the present microconch by more rounded flanks and a depressed as well as highly evolute body chamber. *H. mutans* (Collignon 1958, pl. XXIX, fig. 127) is unrelated because of the presence of more number of weak ribs and we excluded it. *O. aff. obtusicoelata* (Collignon 1958, pl. XXIX, fig. 133) and *O. ushas* (Collignon 1958, pl. XXIX, fig. 131) described from the Middle Callovian of Madagascar are synonymised as macroconchs of *O. obtusicoelata*. Cariou et al. (1996, fig. 7) described *O. aff. ankoboensis* from the Middle Callovian of the Spiti Shales, Himalayas. It resembles the inner whorls of the present species in coiling and ornamentation and is therefore synonymised here. *H. omphaloides* of Cariou et al. (1996, fig. 6) is similar to the present microconch and also synonymised.



◀ **Fig. 12** *Obtusicosites obtusica* (Waagen) [m]. **a–c** Allotype; complete specimen with lappet (GSI no. 2030; Waagen 1875, pl. XXXVII, fig. 2a,b); lateral, ventral and apertural views; from ‘*Perisphinctes anceps* beds’ of Vanda. **d–f** Adult with trace of a broken lappet; (GSI no. 2035; Waagen 1875, pl. XXXVIII, fig. 4a); lateral, apertural and ventral views; from ‘*Perisphinctes anceps* beds’ of Keera (Bed nos. 5–7, see fig. 3). **g, h** Adult phragmocone; GSI no. 2036 (Waagen 1875, pl. XXXVIII, fig. 4b,c); lateral and apertural views; Golden Oolite, Keera (Bed no. 2). **i, j** Specimen with lappet; JUM/OO/14; lateral and ventral views; locality and stratigraphy unknown. **k, l** Adult with preserved lappet; JUM/OO/15; lateral and ventral views; Bed 8; Jumara (see Fig. 2). Scale bar 2 cm. Arrows indicate the lappet. X marks the beginning of body chamber

Obtusicosites devi (Spath, 1931) (Fig. 13a–m)

v* 1931. *Obtusicosites devi*, Spath, parts, pl. LII, fig. 5a,b; pl. LIV, fig. 1a,b [M]

v 1931. *Hubertoceras?* sp. nov., Spath pl. LXXIX, fig. 4a,b [M]

v 1931. *H. hubertus*, Spath, parts, pl. LII, fig. 7; pl. LXIX, fig. 4a,b; pl. LVI, fig. 4; pl. LXVIII, fig. 11 [M]

Holotype: Specimen GSI type no. 16076[M]

Measurements: see Table 2

Remarks: Spath (1931) described many *Obtusicosites* and *Hubertoceras* species from higher stratigraphic horizons, i.e. his ‘*athleta* beds’ (Upper Callovian). These forms have flattish flanks with a shallow umbilicus and more number of ribs compared to the older *O. obtusica* which has its highest abundance in the Middle Callovian. These ‘*athleta*’ species were assigned to *O. devi* of Spath. They included both macroconchs and microconchs.

Within the macroconch, we synonymised Spath’s *O. devi* (pl. LII, fig. 5a,b, pl. LIV, fig. 1a,b, pl. LVIII, fig. 7a,b) along with one specimen described as *Hubertoceras?* sp. nov. (pl. LXXIX, fig. 7a,b). Some other specimens described by Spath (1931) as *O. devi* are most likely to be related to *O. obtusica* which has less number of strong ribs (for example pl. XLV, fig. 5; pl. LII, fig. 2a,b; pl. LV, fig. 4, and pl. LXV, fig. 3) and were included into *O. obtusica*. Unfortunately no specimen had an adult body chamber preserved. The holotype of *O. devi* is an adult septate specimen with half of the outer whorl (missing) occupied by the adult body chamber as evident from the trace of the umbilical seam. While describing the differences of this species with *O. obtusica*, Spath (1931) correctly observed that *O. devi* had a weaker and denser costation of both primary and secondary ribs. In the adult phragmocone, *O. devi* has more ribs ($P = 14, S = 38$) than *O. obtusica* ($P = 12, S = 35$).

O. devi also differs from *O. obtusica* in having more evolute shell. We noted the ontogenetic change in the nature of ribbing pattern of *O. obtusica*: the ribs become

more numerous ($P = 13, S = 33$) in the adult body chamber of *O. obtusica* compared to the preceding whorl ($P = 12, S = 28$). This tendency of an increase in the number of primaries in the adult *O. obtusica* already appears at an early stage of *O. devi*. The evolutionary mechanism perhaps involves heterochronic paramorphism, more specifically acceleration. Spath (1931) erroneously mentioned that the adult body whorl of *O. obtusica* is smooth, but he did not provide any specimen to support this statement. We described the adult body whorl of *O. obtusica* on the basis of newly discovered adult specimens which is thoroughly ribbed up to the preserved end and show no sign of a disappearance of ornamentation. We also believe that the adult body whorl of *O. devi* also is thoroughly ribbed (more number of ribs this time).

The holotype of *Hubertoceras hubertus* (here reproduced Fig. 13l, m) is almost identical to the septate macroconch of *O. devi* (Fig. 13c, d), but has a denser costation and the branching points of the ribs are higher. It has lappets and diameter is of 70 mm. We consider this specimen as the microconch of *O. devi*. Unfortunately, its locality is unknown and the stratigraphy is doubtful, but similar looking other additional specimens come from the same locality and horizon from where the holotype of the macroconch was reported. They are *H. hubertus* var. *densicostata* and *H. hubertus* var. *rotunda* and are also considered here to be microconchs of *Obtusicosites devi*.

Microconchs of *O. devi* also show a similar change in the ribbing pattern like that as in *O. obtusica*. Ribs are relatively more or numerous ($P = 15, S = 29$). Primaries are relatively weak, less differentiated than secondaries. Notably furcation takes place high on the outer flank. Shell is planulate with a larger diameter ($D = 56$ mm) than in *O. obtusica*.

Genus *Kinkeliniceras* Buckman, 1921

Type species: *Proplanulites kinkelini* Dacque, 1910

Diagnosis: Macroconch medium sized (maximum $D = 139$ mm), involute to less evolute ($U/D = 0.2–0.32$), highly compressed ($W/H = 0.64–0.83$), finely and densely ribbed, strength of primary and secondary ribs not well differentiated. Microconch less evolute, relatively strongly ribbed on body chamber which becomes flexuous in latter part of the whorl. The size ratio of macroconchs and microconchs (M: m) is 2: 1.

Species included: *Kinkeliniceras angygaster* and *Kinkeliniceras kinkelini*.

Stratigraphical and geographical occurrences: Lower to Upper Callovian; Kutch, Madagascar and Tanzania.

Kinkeliniceras angygaster (Waagen, 1875) (Figs. 6c, 14, 15a–k, and 16a–l)

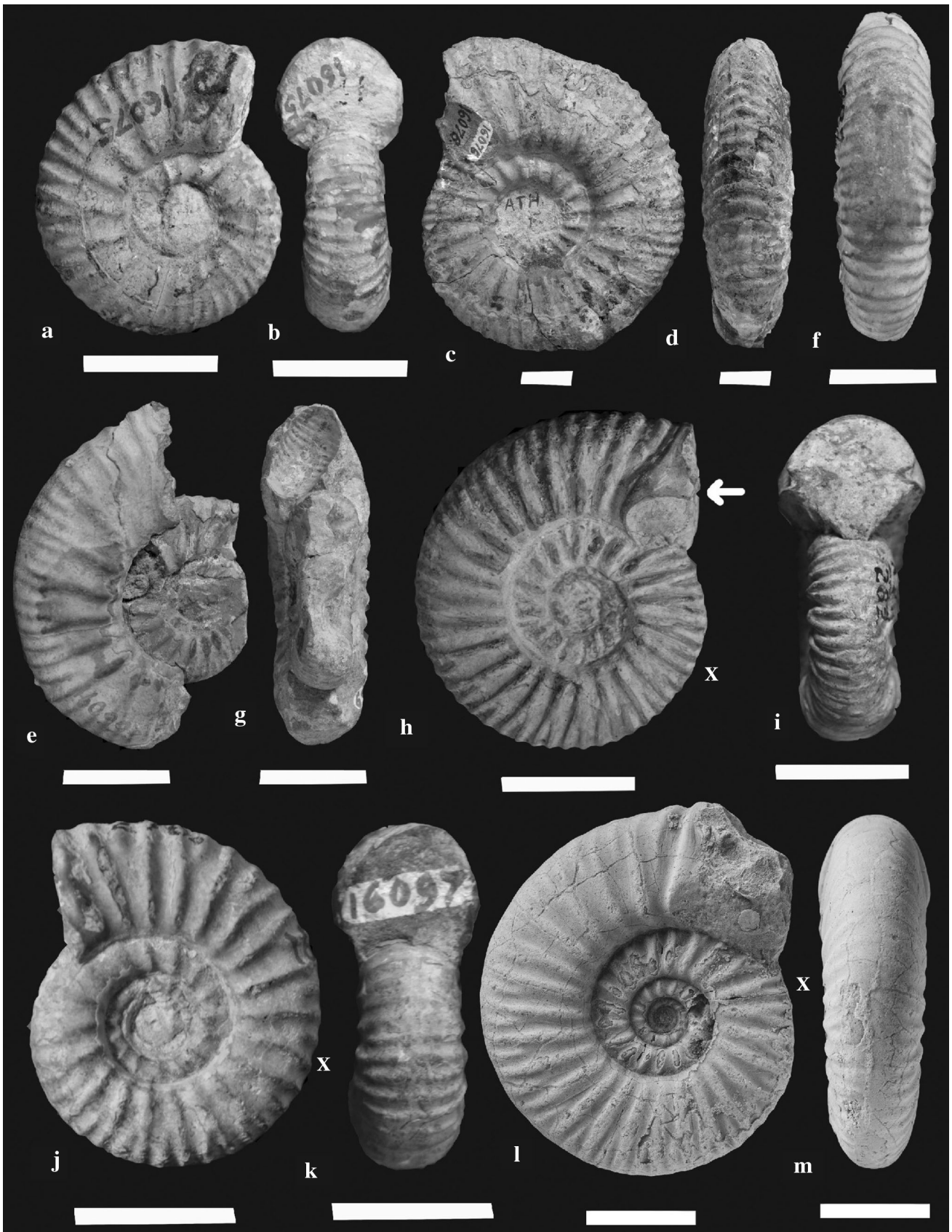
Table 2 Measurements of all macroconchs and microconchs of *Obtusicosites obtusicosta* and *O. devi*

Specimen no	Description	D	U	W	H	P	S	RW	RS	U/D	W/H
<i>Obtusicosites obtusicosta</i>											
JUM/J/OO/1[M]	Body chamber	165	60			13	33	5	6.5	0.36	
	Phragmocone	141	52	42	58	12	28	4.26	5.77	0.37	0.72
JUM/J/OO/2[M]	Phragmocone	136	48.5	44	54	12	32	6.25	5.8	0.36	0.81
JUM/J/OO/3[M]	Phragmocone	92	34	36.5	38	10	25	4.87	5.43	0.37	0.96
JUM/J/OO/4[M]	Phragmocone	91	34	33	36	9	25	4.55	5.68	0.37	0.92
JUM/J/OO/5[M]	Phragmocone	117	44.5	39	44	11	30	4.6	5.01	0.38	0.89
	Innerwhorl	57.5	23	20	22.5	9				0.40	0.89
	Innerwhorl	30	11.7	11.6	10.7					0.39	1.08
JUM/J/OO/6[M]	Phragmocone	85	33	30	33	14		4.3	4.5	0.39	0.91
JUM/J/OO/7[M]	Phragmocone	94.5	36	34.6	36.7			4	5.5	0.38	0.94
	Innerwhorl	65	26	29	27	9		2.8	4	0.40	1.07
JUM/JA/OO/8[M]	Phragmocone	53	19	24	22	9		2.77	4.33	0.36	1.09
JUM/J/OO/9[M]	Phragmocone	90	35	29.7	35			3	4.5	0.39	0.85
JUM/J/OO/10[M]	Innerwhorl	40.6	16.2	15	15	12	26	1.8	2.4	0.40	1.00
JUM/J/OO/11[M]	Innerwhorl	35	13	14.7	15.5	9	21	1.32	2.2	0.37	0.95
JUM/JA/OO/12[M]	Innerwhorl	50	19	16.2	18	14	29	2	2.8	0.38	0.90
JUM/J/OO/13[M]	Innerwhorl	48	20	17.8	19					0.42	0.94
	Innerwhorl	28.4	12	9.5	9.21	7		1.4	2	0.42	1.03
GSI 2032 [M] ^a	Holotype, phragmocone	157	51	54	66	11	37	8.21	7.36	0.32	0.82
	Innerwhorl	116	39	45	54	11	33	6.47	5.4	0.34	0.83
GSI 2033 [M]	Body chamber	159	60	56	68	12	35	6.42	5.86	0.38	0.82
	Phragmocone	73	29	25.8	28.5					0.40	0.91
GSI 2034 [M]	Phragmocone	77	28.5	29	33.3	8	23	5.3	6.5	0.37	0.87
	Innerwhorl	57	20	22	24	8	23	4.89	6.02	0.35	0.92
GSI 16073[M]	Phragmocone	73	24	26	30	10		3.75	4.61	0.33	0.87
	Innerwhorl	54.5	18	22.5	22.6	9		2.2	3.22	0.33	1.00
	Innerwhorl	34	11	15	15	8		1.8	2.11	0.32	1.00
GSI 16077[M]	Phragmocone	124	41.5	43	52	11		5.6	7.5	0.33	0.83
	Innerwhorl	97	32	33.5	38	11	28	4.8	6.24	0.33	0.88
GSI 16078[M]	Phragmocone	70	27	24	26	10	24	4	5	0.39	0.92
	Innerwhorl	35	11.8	14	14	9		2.36	3	0.34	1.00
GSI 16087[M]	Phragmocone	57	19	24	23	9		3.2	4.3	0.33	1.04
	Innerwhorl	41	12	16.8	17	8	29	2	3.05	0.29	0.99
GSI 16080[M]	Phragmocone	69	25	25	24	10	26	4.28	4.7	0.36	1.04
	Innerwhorl	55	22	23	22	10	28	3.5	3.7	0.40	1.05
GSI 16082[M]	Phragmocone	91	32	35	35	10	21	4.85	5.78	0.35	1.00
	Innerwhorl	50	22	22	19					0.44	1.16
GSI 16086c[M]	Phragmocone	76	25	25	25.5			1.7	1.34	0.33	0.98
	Innerwhorl	58.6	18	17.3	17					0.31	1.02
JUM/J/OO/14[m]	Body chamber	47.66	20	14.8	16.52	11	26	2.35	2.68	0.42	0.89
	Phragmocone	37.8	14.6	11.8	14.7	11	25	1.74	2.3	0.39	0.80
JUM/K/OO/15[m]	Body chamber	45	17.6	17.3	16.83	10	19	2	2.72	0.39	1.03
JUM/U/OO/16[m]	Phragmocone	49.6	18.5	20	21.7	8	24	2.3	3.77	0.37	0.92
	Innerwhorl	37	13	14.7	16	9	26	1.48	2.34	0.35	0.92
JUM/U/OO/17[m]	Phragmocone	43	16.4	14.9	16.6	11	24	2.55	3.12	0.38	0.90
	Innerwhorl	36	14	11	13	12	23	1.5	2.2	0.39	0.85
JUM/JA/OO/18[m]	Phragmocone	53	23.7	13.5	17.6	13	26	2.18	3.25	0.45	0.77
	Innerwhorl	44	19	14.3	15	12	25	2	2.3	0.43	0.95

Table 2 continued

Specimen no	Description	D	U	W	H	P	S	RW	RS	U/D	W/H
JUM/U/OO/19[m]	Phragmocone	40.7	16	14.3	15	12	25	2	2.4	0.39	0.95
	Innerwhorl	31	12.6	13	12	11	24	1.64	2.2	0.41	1.08
JUM/U/OO/20[m]	Phragmocone	42.3	13.7	16.2	18.3	9	20	2.2	3.3	0.32	0.89
	Innerwhorl	32.6	11.2	11.9	13.7	8	16	1.9	2.62	0.34	0.87
JUM/U/OO/21[m]	Body chamber	38	15	14.2	15.3	10	19	2.13	3.18	0.39	0.93
JUM/U/OO/22[m]	Innerwhorl	36	12	14.3	15.5	9	17	2.3	3	0.33	0.92
		27	9.6	11.8	12.5	8	16	2	2.8	0.36	0.94
JUM/J/OO/23[m]	Innerwhorl	37	13.5	12	14.8	11	24	2	2.6	0.36	0.81
	Innerwhorl	29	10	10.8	11.6	11	22	1.7	2.3	0.34	0.93
JUM/J/OO/24[m]	Innerwhorl	37	11.5	13.8	16.3	8	17	2	2.8	0.31	0.85
		29	9.6	11.6	13.7	8	18	1.8	2.3	0.33	0.85
JUM/U/OO/25[m]	Phragmocone	45	21	17.5	18.5	12	23	1.92	2.2	0.47	0.95
	Innerwhorl	23.8	9.3	10.5	9.6	13		1	1.3	0.39	1.09
JUM/J/OO/26[m]	Innerwhorl	30.17	10.4	10.5	12			1.4	1.7	0.34	0.88
JUM/J/OO/27[m]	Phragmocone	39.2	17	12.8	15.5	11		2.2	2.5	0.43	0.83
JUM/J/OO/28[m]	Phragmocone	43	22.7	17.9	17.6					0.53	1.02
	Innerwhorl	24.14	12.2	8.6	9.7	11		0.8	1.3	0.51	0.89
	Innerwhorl	12.6	6.7	5.1	4.3	10		0.5	0.8	0.53	1.19
	Innerwhorl	6.8	3.3	2.8	2.32					0.49	1.21
GSI 2030[m] ^a	Allotype, body chamber	49.5	18	13	17	13	23	2.64	2.87	0.36	0.76
	Phragmocone	38	16	11.5	14	13	21	2.23	2.58	0.42	0.82
GSI 2035[m]	Body chamber	48.4	16	16	20	11	23	2.42	2.59	0.33	0.80
	Phragmocone	35	11.5	13.6	16	10	20	2.2	2.35	0.33	0.85
GSI 16084[m]	Body chamber	45.7	17.6	14	17	10	21	2.4	3.2	0.39	0.82
	Phragmocone	37	15	14.5	15	9	21	2.13	2.9	0.41	0.97
GSI 2036[m]	Body chamber	47.2	17.3	18	19.3	11	21	2.25	3.46	0.37	0.93
	Phragmocone	36	13	12.7	14	10	19	1.75	3.12	0.36	0.91
GSI 16079[m]	Phragmocone	38	15	10	11	10	22	2.2	2.47	0.39	0.91
	Innerwhorl	30	11	10.5	11					0.37	0.95
	Innerwhorl	21	9	8.23	7.88	8		1.44	1.7	0.43	1.04
	Innerwhorl	14.5	6	4.2	4					0.41	1.05
<i>Obtusicosites devi</i>											
GSI 16076[M] ^a	Holotype, phragmocone	136	47	36	54	14	38	3.69	4.34	0.35	0.67
	Innerwhorl	105	41	34	42	14	38	3.44	4.2	0.39	0.81
GSI 16099[M]	Phragmocone	71	27	19	24			2.5	3.6	0.38	0.79
	Innerwhorl	37	14	12	15			1.68	1.42	0.38	0.80
GSI 16075[M]	Phragmocone	46.5	18	19.6	18.74	9	24	2.7	4	0.39	1.05
	Innerwhorl	36	14	14.5	15	10	26	2	3.3	0.39	0.97
GSI 16098[m]	Body chamber	56	22	20	20	15	29	2.46	2.62	0.39	1.00
	Innerwhorl	44	18	15.8	16	13	27	2	2.2	0.41	0.99
GSI 16097[m]	Body chamber	37	15.7	13.4	14	12	19	1.67	1.99	0.42	0.95
	Innerwhorl	29	12	11.5	11	11	22	1.48	1.81	0.41	1.05
NHMUK C 7686[m]	Body chamber	73	27.7	21.9	24.82	15	30			0.38	0.88

^a The holotype



◀ **Fig. 13** *Obtusicosites devi* (Spath) [M]. **a, b** Phragmocone; GSI no. 16075 (Spath 1931, pl. LII, fig. 5a,b); lateral and apertural views; 'athleta or anceps beds' of Fakirwadi. **c, d** Holotype; adult phragmocone; GSI no. 16076 (Spath 1931, pl. LIV, fig. 1a,b); lateral and ventral views; 'athleta' beds' of Fakirwadi. **e–g** Phragmocone; GSI no. 16099 (Spath 1931, pl. LXXIX, fig. 4a,b); lateral, ventral and apertural views; 'athleta beds' of Fakirwadi. **h–m** [m] **h, i** Adult with partly broken lappet; note denser costation; GSI no. 16098 (Spath 1931, pl. LXIX, fig. 4a,b); lateral and apertural views; 'athleta beds' of Fakirwadi. **j, k** Partly preserved adult body chamber; GSI no. 16097 (Spath 1931, pl. LVI, fig. 4); lateral and apertural views; 'athleta beds' of Fakirwadi. **l, m** Adult with broken lappet; NHMUK no. C 7686 (Spath 1931, pl. LII, fig. 7); lateral and ventral views; probably 'anceps beds', locality unknown. Scale bar 2 cm. Arrows indicate the lappet. X marks the beginning of body chamber

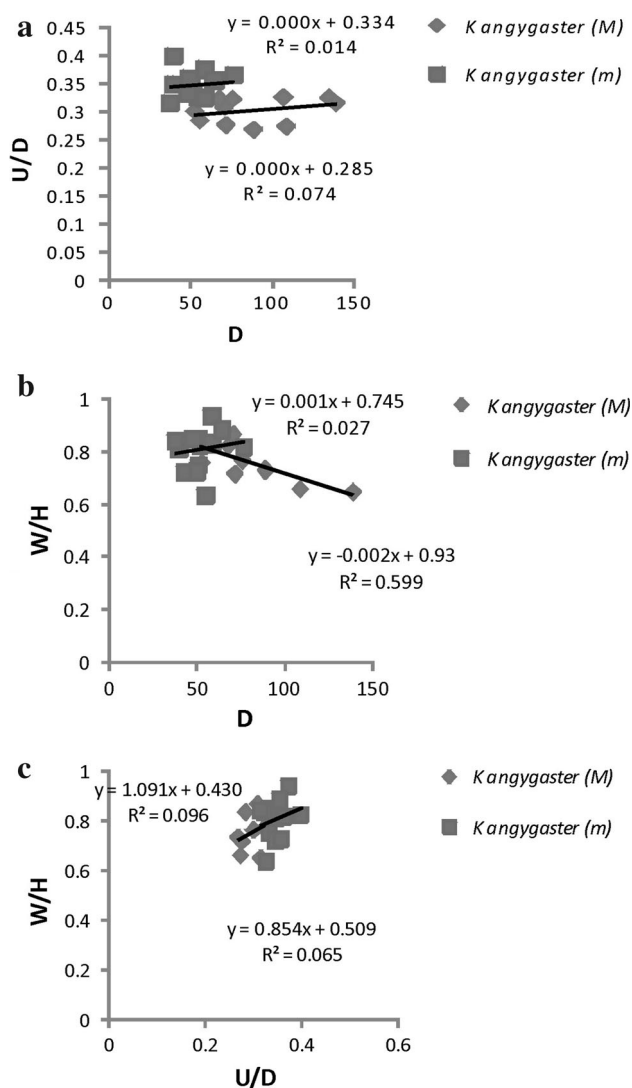


Fig. 14 Bivariate analyses of *Kinkeliniceras angygaster* (Waagen). *M* Macroconch, *m* microconch. **a** Degree of involution versus diameter. **b** Degree of inflation versus diameter. **c** Degree of inflation versus degree of involution

v* 1875. *Perisphinctes angygaster*, Waagen, p. 148, pl. XXXIX, figs. 2a,b [M]

v 1931. *Kinkeliniceras angygaster*, Spath, pl. XLVI, fig. 3; pl. LIII, figs. 4a,b; Pl. LXI, figs. 1, b [M]

v 1931. *Kinkeliniceras catillus*, sp. nov., Spath, pl LV, fig. 1, pl LVIII, figs. 6a,b [M]

v 1931. *Kinkeliniceras discoideum* sp. nov., Spath, pl. LV, fig. 3 [M]

v 1931. *Kinkeliniceras varuna* sp. nov., Spath, pl. LIV, fig. 5a,b; pl. LVIII, figs. 2a,b; pl. LX, figs. 3a,b. [m]

v 1931. *Kinkeliniceras Krishna* sp. nov., Spath, pl. LVIII, fig. 1, pl. LXIII, fig. 2 [M].

1958. *Kinkeliniceras angygaster* (Waagen), Collignon, pl. XXIX, fig. 134.

1958. *Kinkeliniceras varuna* (Spath), Collignon, pl. XXX, fig. 139.

1958. *Kinkeliniceras discoideum* (Spath), Collignon, pl. XXXI, fig. 142.

Holotype: Specimen GSI type no 2038[M]

Measurements: see Table 3

Description: Macroconch: The maximum preserved diameter of the adult shell is 139 mm. The shell is relatively not very evolute and compressed (Fig. 14).

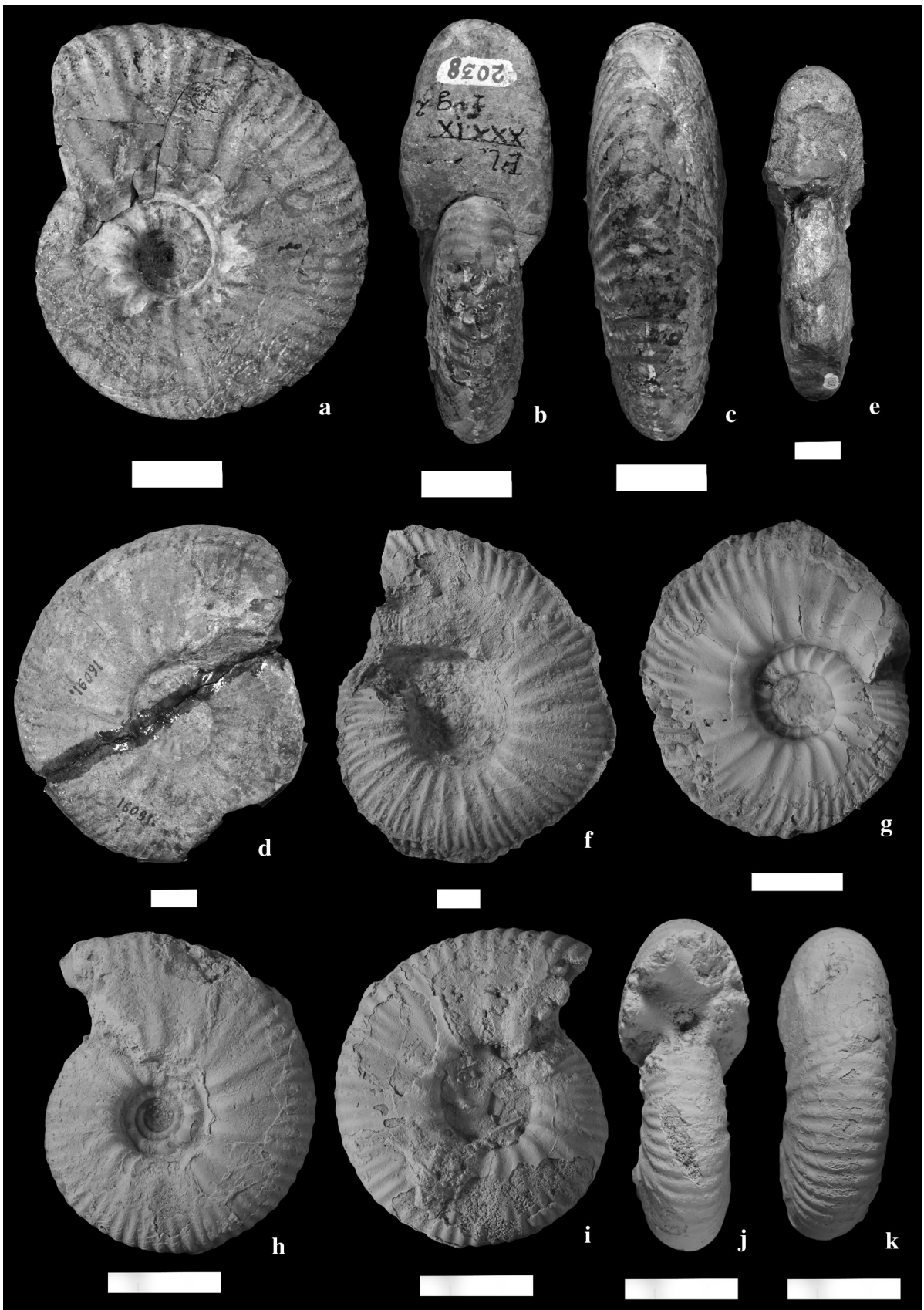
Inner whorls ($D = 56$ mm) are involute ($UID = 0.28$) and compressed ($W/H = 0.83$). Umbilicus is narrow and steeply inclined with distinct umbilical wall. The primary ribs are strong and thick ($P = 9$) and furcate at or above the mid-flank into two to three relatively weak secondaries ($S = 33$). Solitary ribs are placed irregularly.

At diameters between 68 and 89 mm, the shell is slightly evolute to involute (UID ranges from 0.32 to 0.26) and compressed ($W/H = 0.86$ –0.71). Umbilicus is deep and narrow. Primary ribs are weak and slightly flexuous. Ribbing pattern remains same with forwardly projected secondaries ($P = 8$ –12 and $S = 32$ –33).

At adult phragmocone ($D = 135$ –139 mm), shell is slightly evolute ($UID = 0.31$ –0.32). Ontogenetically, shell becomes more compressed during growth than the earlier ($W/H = 0.83$ –0.64). Ribs are numerous ($P = 12$ and $S = 44$) and relatively weak.

Unfortunately, large adult specimens with preserved body chamber are not available, changes on the adult body whorls are therefore not known. However, one smaller adult variant (Spath 1931, pl. LXI, fig. 1a,b) with a diameter of 150 mm shows that primaries become excessively thick and form bullae near the inner flank on the body whorl. Other characters are more or less remain same (e.g. example number of ribs and nature of furcation etc.). The body chamber occupies almost the whole outer whorl.

Spath (1931) illustrated the suture line (pl. LXIII, fig. 2) of *K. krishna* (here synonymised) which we have refigured



◀ **Fig. 15** *Kinkeliniceras angygaster* (Waagen) [M]. **a–c** Holotype; phragmocone; note shell is involute and primary ribs are slightly flexuous near the end; GSI no. 2038 (Waagen 1875, pl. XXXIX, fig. 2a,b); lateral, apertural and ventral views; from ‘*Perisphinctes anceps* beds’ of Keera (=Bed nos. 5–7, see Fig. 3). **d, e** Adult phragmocone; GSI no. 16091 (Spath 1931, pl. LV, fig. 3); lateral and apertural views; from ‘*anceps* beds’ of Fakirwadi. **f** Phragmocone; JUM/KA/1; lateral view; locality and stratigraphy unknown. **g** Phragmocone; JUM/KA/4; lateral view; locality and stratigraphy unknown. **h–k** Inner whorls; JUM/KA/3; laterals, aperture and ventral views; locality and stratigraphy unknown. *Scale bar 2 cm*

here (Fig. 6c). Spath (1931) correctly noticed that the first lateral lobe was slightly shorter than the siphonal lobe. He admitted that this cannot use as specific character because it varies from specimen to specimen. In one of our specimens, the first lateral lobe is longer than the siphonal lobe, but the complete sutural pattern was not preserved in this specimen.

Microconch: The maximum diameter of the shell (GSI type-16094, here reproduced as Fig. 16f, g) is 76.5 mm. The adult phragmocone stage ($D = 50$ mm), the shell is evolute and compressed ($U/D = 0.36$ and $W/H = 0.72$). The bifurcating nature of the ribs already appears at the late phragmocone stage with few intercalated solitaries. Primary and secondary ribs at the end of the adult phragmocone diameter are comparatively dense ($P = 15$ and $S = 33$).

Adult shell varies in diameter from 51 to 76.5 mm, U/D ranges from 0.3 to 0.36 and W/H ranges from 0.75 to 0.88. The body whorl is thoroughly ribbed ($P = 11–15$ and $S = 26–34$). Primaries are less strong, ribbing pattern essentially bifurcating, rectiradiate to slightly prorsiradiate. However, in one variant (Fig. 10i, j) ribs are slightly flexuous and secondaries pass over the venter rursiradiately. Flanks are flat, furcation takes place at the middle of the flank.

Adult body chamber occupies more than half of the outer whorl. Peristome preserved with terminal constriction and narrow long lappets.

Remarks: Spath (1931) described 10 species in the genus *Kinkeliniceras*. After the present revision only two species remain, i.e. *K. angygaster* and *K. kinkelini*. *K. cattilus*, *K. discoideum* and *K. krishna* of Spath are synonymised as macroconchs of *K. angygaster*. *K. varuna* is synonymised as the microconch of *K. angygaster*. *K. indra* is synonymised with *K. kinkelini*. We excluded *K. subwaageni*, *K. crassiplanula* and *K. pseudomaya* from the genus *Kinkeliniceras*. Spath (1931) was uncertain about the status of *K. subwaageni* since the holotype was a doubtful specimen. It is unrelated to *K. angygaster* because it is evolute, more compressed ($U/D = 0.35$ and $W/H = 0.49$) and the body chamber is smooth or weakly ribbed at the beginning.

It may be an *Indosphinctes* Spath. *K. crassiplanula* is transitional to *O. obtusicosta* (synonymised here) because of its thick bullae-like primary ribs. *K. pseudomaya* is also unrelated and Spath found similarities with *Mayaites* Spath which is exclusively of Oxfordian age (see Alberti et al., 2015).

Collignon (1958) described *K. cattalai* (pl. XXIX, fig. 136) from the Middle Callovian of Madagascar. The species is characterized by its fine ornamentation and relatively weak ribbing. It is a medium-sized species with a preserved shell diameter is of 61 mm. It differs from the present species by its very dense, fine ribbing and uncoiling trend visible in the nature of umbilicus. However, it resembles the present species regarding the degree of involution ($U/D = 0.34$), inflation ($W/H = 0.77$) and number of primary ribs ($P = 20$). Another species of Collignon (1958, pl. XXIX, fig. 135) as *Kinkeliniceras kinkelini* is evolute and has a bifurcating ribbing pattern. It resembles the microconch of *O. obtusicosta* (synonymised here). He also described *Kinkeliniceras crassiplanula* (1958, pl. XXX, fig. 140) which is a large adult phragmocone (166 mm) and comparable with *Sivajiceras paramorphum* (synonymised here).

Kinkeliniceras kinkelini (Dacque, 1910) (Fig. 17a–l)

v* 1931. *Kinkeliniceras kinkelini*, Spath, pl LVIII, figs. 3a,b, pl LXII, figs. 7a,b, 10.

1931. *Kinkeliniceras indra* sp. nov., Spath, pl LIX, fig. 10a,b.

1958. *Kinkeliniceras kinkelini*, (Dacque), Collignon, pl. XXX, fig. 137.

1958. *Kinkeliniceras indra*, (Waagen), Collignon, pl. XXX, fig. 138.

Holotype: Specimen pl. V, fig. 1 of Dacque, 1910 (*Repository information is not known*)

Measurements: see Table 3

Remarks: The holotype of the present species comes from East Africa (Dacque and Krenkel 1909) and Spath (1931, pl. LXII, fig. 7 a,b) found a similar specimen from Kutch. The latter Kutch specimen is 66 mm in diameter and is involute ($U/D = 0.29$) and compressed ($W/H = 0.8$). The present species differs from *K. angygaster* in the absence of rectiradiate, unprojected ribs and the broader ventral area (Spath, 1931, p. 308). *K. indra* is also similar to the present species having a dense costation and is synonymised here. Spath (1931) compared one of the variants (*K. kinkelini* var. *senilis*; Spath 1931, pl. LVIII, fig. 3a,b; here reproduced as Fig. 17a–c) of the present species to *K. angygaster*. The former differs from the latter in having a wider ventral area and rectiradiate secondary ribs. In fact, the

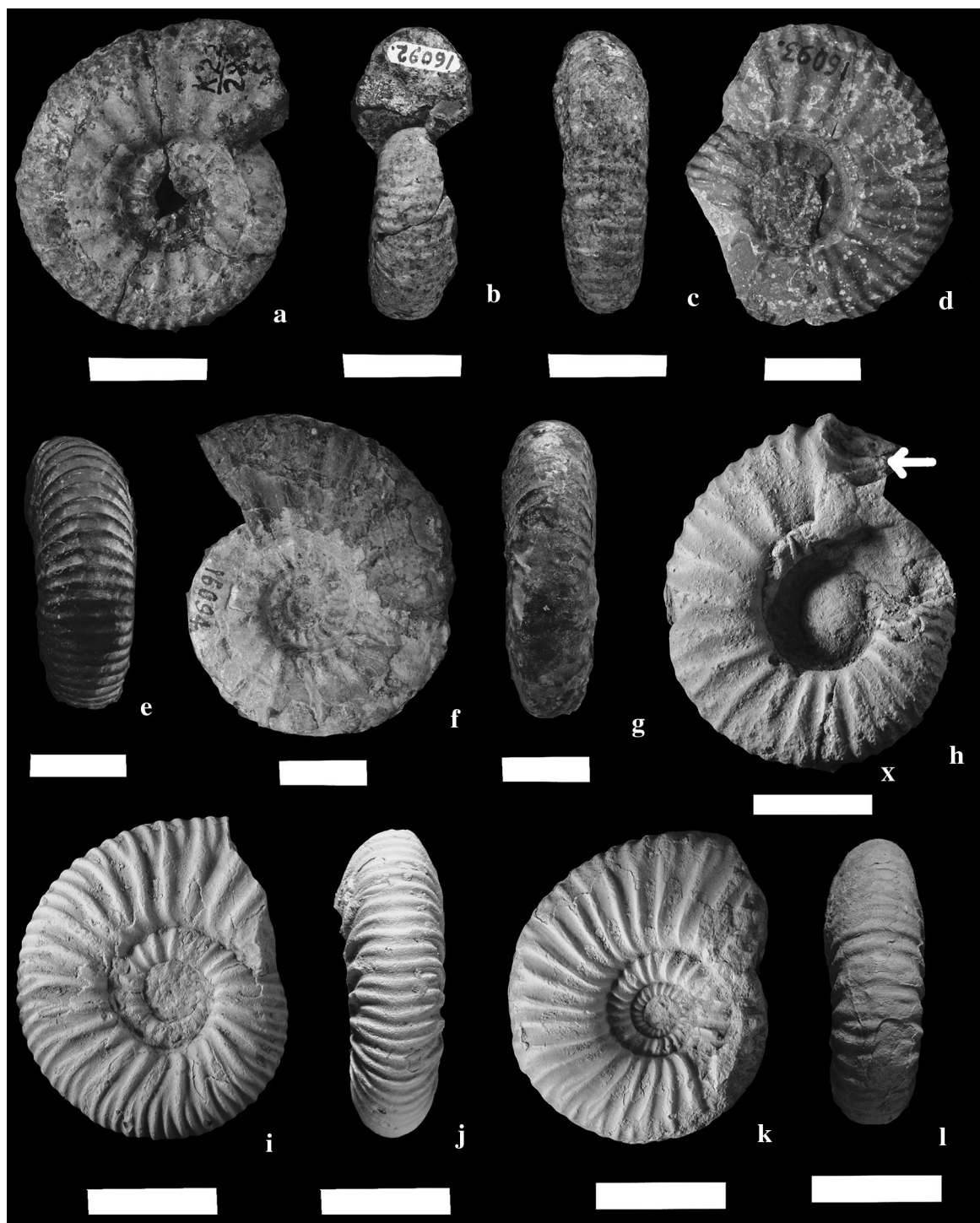


Fig. 16 *Kinkeliniceras angygaster* (Waagen) [m]. **a–c** Adult phragmocone; GSI no. 16092 (Spath 1931, pl. LIV, fig. 5a,b); lateral, apertural and ventral views; from ‘*Perisphinctes anceps*’ beds of Fakirwadi. **d, e** Adult phragmocone; GSI no. 16093 (Spath 1931, pl. LVIII, fig. 2a,b); lateral and ventral views; from ‘*anceps* beds’ of Fakirwadi. **f, g** Adult phragmocone; GSI no. 16094 (Spath 1931, pl. LX, fig. 3a,b); lateral and ventral views; from ‘*Anceps* beds’ of

Fakirwadi. **h** Adult with preserved lappet; note narrow long lappet preceded by the terminal constriction; JUM/KA/5; lateral view; Medisar, Jhura. **i, j** Adult phragmocone; JUM/KA/7; lateral and ventral views; Bed 11; Jumara (see Fig. 2). **k, l** Adult phragmocone; JUM/KA/8; lateral and ventral views; locality and stratigraphy unknown. Scale bar 2 cm. Arrows indicate the lappet. X marks the beginning of body chamber

Table 3 Measurements of all macroconchs and microconchs of *Kinkeliniceras angygaster* and *K. kinkelini*

Specimen no	Description	D	U	W	H	P	S	RW	RS	U/D	W/H
<i>Kinkeliniceras angygaster</i>											
JUM/J/KA/1[M]	Phragmocone	135	44				43	4.48	5	0.33	
	Innerwhorl	107	35			16	41	3.14	3.94	0.33	
JUM/J/KA/2[M]	Phragmocone	71	22	26	30	8	32	2.77	4.03	0.31	0.87
JUM/J/KA/3[M]	Phragmocone	56	16	20	24	9	33	2.15	2.76	0.29	0.83
JUM/J/KA/4[M]	Phragmocone	68	22	23	28	11	33	2.67	3.08	0.32	0.82
GSI 2038[M] ^a	Holotype, phragmocone	89	24	30	41	10	32	3	4.5	0.27	0.73
	Phragmocone	72	20	24	33.5	9	33	2.73	3.86	0.28	0.72
GSI 16091[M]	Phragmocone	139	44	37	57	12	44	3.5	3.08	0.32	0.65
	Phragmocone	109	30	31	47	11	35	3.9	4.2	0.28	0.66
GSI 16096[M]	Phragmocone	76	24.6	25	32.6	12		2.6	3.3	0.32	0.77
	Innerwhorl	53	16	19	25	13		1.78	2.09	0.30	0.76
JUM/J/KA/5[m]	Body chamber	51	17	15	20	12	26	2.5	3.5	0.33	0.75
	Phragmocone	43	15	13	18	13	30	2.4	3.3	0.35	0.72
JUM/J/KA/6[m]	Phragmocone	52		17	20	12	24	2.6	3.4		0.83
JUM/J/KA/7[m]	Phragmocone	51	17	17	20	15	33	2.8	3.3	0.33	0.85
	Inner whorl	40	14	13	16	13	31	2.4	3	0.35	0.81
JUM/J/KA/8[m]	Phragmocone	50	18	16	22	15	30	2	2.8	0.36	0.73
	Innerwhorl	40	16	14	17	14	27	2	2.5	0.40	0.82
JUM/J/KA/9[m]	Body chamber	55	18	14	22	15	27	2	3.5	0.33	0.64
J.H. Smith Colln. No. 844	Body chamber	150	31.5	44	61.5					0.21	0.70
GSI 16092[m]	Phragmocone	58.5	22	23	24	11	28	2.6	2.81	0.38	0.94
	Innerwhorl	48	16	17	20	10	29	2.3	3	0.33	0.85
GSI 16094[m]	Phragmocone	76.5	28	25	30	11		3.7	4.6	0.37	0.82
	Inner whorl	58.5	19	20	24	11		3.2	4.1	0.32	0.83
GSI 16093[m]	Phragmocone?	64.5	23	23	26	13	29	3.3	2.95	0.36	0.88
	Inner whorl	38	12	16	19	9		1.82	2.2	0.32	0.84
<i>Kinkeliniceras kinkelini</i>											
JUM/J/KK/1	Phragmocone	66	22	23	29	8	33	3	4.5	0.33	0.79
	Inner whorl	51	17	18	24	9	29	3	4.5	0.33	0.75
JUM/J/KK/2	Inner whorl	38	12	14	16	9	25	2	3	0.32	0.88
	Inner whorl	29	11.5	12	11.3	8	21	1.72	2.6	0.40	1.03
GSI 16096a	Phragmocone	69	21	19	29	9	29	3	3.4	0.30	0.66
	Inner whorl	52	17	19	23.4	8	31	2.6	3.2	0.33	0.79

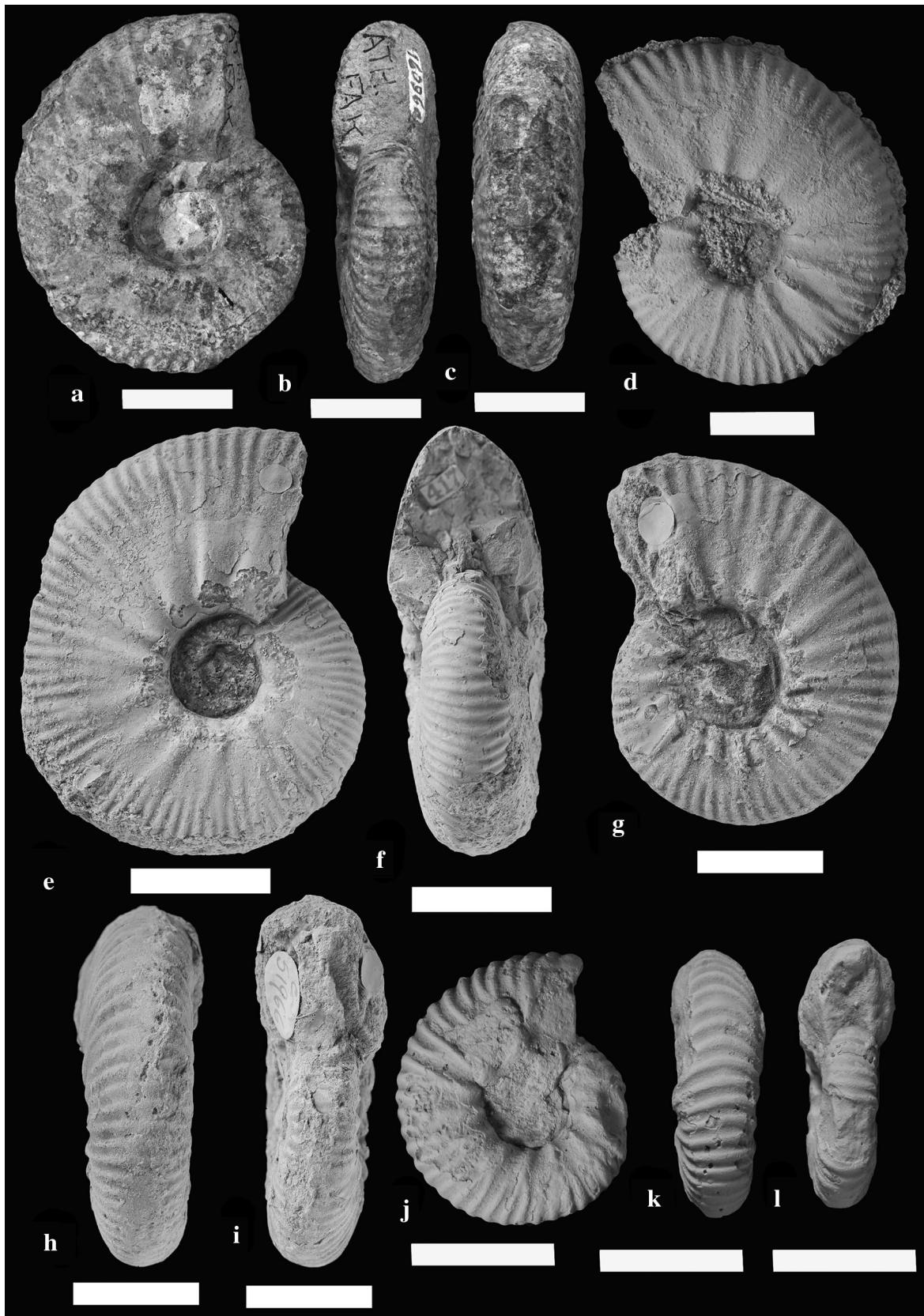
^a The holotype/other type

variant might be a small adult (70 mm). It shows ontogenetic changes in the ribbing pattern. Bullae-like primary ribs of the early inner whorls weaken at the end-phragmocone which is marked by the egression of the body chamber. On the body whorl, ribs are few ($P = 8-9$ and $S = 29-32$) and undifferentiated.

All present specimens are septate and resemble the inner whorls of Spath's examples. Because of its smaller size, fine ribbing, the present species is assigned separately from *K. angygaster*. Collignon's *K. kinkelini* (1958, pl. XXX, fig. 137) and *K. indra* (1958, pl. XXX, fig. 138) are similar to the present species and synonymised here.

Discussion

Spath (1931) described many species within the five genera *Sivajiceras* Spath, *Obtusicostrites* Buckman, *Hubertoceras* Spath, *Kinkeliniceras* Buckman and *Cutchisphinctes* Spath from the Upper Bathonian and entire Callovian of Kutch. He also grouped all these genera within the subfamily Proplanulitinae of the Boreal Province. Callomon (1993) was the first to comment that the so-called Kutch proplanulitins were perhaps phylogenetically unrelated to the European Proplanulitinae sensu stricto and might constitute an endemic lineage, but he never established this



◀ **Fig. 17** *Kinkeliniceras kinkelini* (Dacque). **a–c** Adult phragmocone; note fine primary and secondary ribs; GSI no. 16096a (Spath 1931, pl. LVIII, fig. 3a,b); lateral, apertural and ventral views; from ‘*athleta* beds’ of Fakirwadi. **d** Adult phragmocone; JUM/KK/1; lateral view; locality and stratigraphy unknown. **e–f** Inner whorls; NHMUK no. C 51967 (Spath 1931, pl. LIX, fig. 10a,b); lateral and apertural views; “*anceps* beds ‘(middle zone)’ of east Jooria”. **g–i** Young specimen; NHMUK no. C 51966 (Spath 1931, pl. LXII, fig. 10); lateral, ventral and apertural views; from ‘*athleta* beds’ of Keera (Bed nos. 9–10, see Fig. 3). **j–l** Inner whorls; JUM/KK/2; lateral, ventral and apertural views; locality and stratigraphy unknown. *Scale bar 2 cm*

hypothesis. We here follow Callomon’s notion to revisit the Kutch genera. We revised the taxa based on specimens archived in the Geological Survey of India, the Natural History Museum, U.K., as well as additional material collected by us from different sections in the mainland of Kutch. We examined the group based on new information about intraspecific variability and sexual dimorphism within a biological species. We altogether recognized seven species within three genera. Roy et al. (2007) recently described *Sivajiceras congener* (Waagen) (M and m) from the Bathonian. We here described six additional species occurring in the Callovian, *S. paramorphum* (Waagen) (M and m), *S. fissum* Sowerby, *Obtusicostrites obtusicostris* (Waagen) (M and m), *O. devi* Spath (M and m), *Kinkeliniceras angygaster* (Waagen) (M and m) and *K. kinkelini* (Dacque). The genera are distinct and show both stratigraphical (see Fig. 4) and morphological (Fig. 18) differences with minor overlapping. It appears that the genus *Obtusicostrites* is generally depressed than the other two genera, but *Obtusicostrites* is equally or slightly less evolute than *Sivajiceras* and occupies an intermediate position between *Sivajiceras* and *Kinkeliniceras*. Thus, the

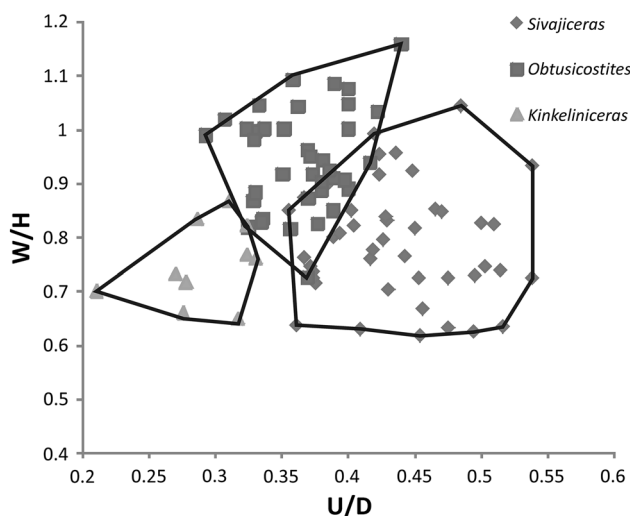


Fig. 18 Bivariate plot of degree of whorl inflation (W/H) against degree of involution (U/D) in macroconchs of the three genera, *Sivajiceras*, *Obtusicostrites* and *Kinkeliniceras*. Note minor overlapping of the distribution between *Sivajiceras* and *Obtusicostrites*

present study supports one universal relationship between shell shape and ornamentation in ammonite’s palaeobiology, which is called Buckman’s Law of Covariation (Westermann 1966; Alberti et al. 2015). This phenomenon suggests that there is a positive correlation between the degree of inflation, involution and the strength of ornamentation. This implies that evolute species are more inflated and strongly ornamented while involute species are compressed and weakly ornamented (Bardhan et al. 2012).

The study of palaeobiogeographic distribution of the Kutch genera and the European proplanulitins reveals clearly a separation of their habitats. Kutch genera were restricted within the Indo-Madagascan Faunal Province, while Proplanulitinae were found mostly in the Boreal Province (Fig. 19). Morphologically, these two groups also have major differences. Indian genera have complex sutural patterns and strong, dense primary ribs in the inner whorls, while these features are lacking in European proplanulitins (Callomon 1993). Because of the palaeobiogeographical and morphological differences, we erected an entirely new subfamily Sivajiceratinae to accommodate the Kutch taxa.

Callomon (1993) found strong similarities between *Sivajiceras congener* and the older *Procerites hians* from Kutch. He even insisted on synonymising the two species. Roy et al. (2007) established that *Procerites* and *Sivajiceras* group of genera formed an evolutionary plexus. They argued that *Sivajiceras* evolved from *Procerites* and subsequently gave rise to *Obtusicostrites* and *Kinkeliniceras* during the Callovian. The evolution involved a complex heterochrony. *Sivajiceras* retains early ornamental features of *Procerites* (neoteny), but also shows the appearance of more advanced features, i.e. the bullae-like primary ribs, and involves peramorphosis. This indicates a complex interplay of heterochronic processes. Neotenus descendant often exhibits novelties (see Bardhan et al. 1994). *Procerites* in Europe was found in older stratigraphic level (Lower Bathonian). In Kutch, it allopatrically gave rise to *Sivajiceras* during the Late Bathonian.

The members of the new subfamily Sivajiceratinae superficially resemble European proplanulitins in some characters, for example, both groups have large macroconchs, evolute shells and bullae-like primary ribs in the phragmocone. These features perhaps prompted Spath (1931) to group the endemic Kutch forms within the Proplanulitinae. Callomon (1993) found also similarities between *Sivajiceras congener* and the European species *Procerites imitator* Buckman. For a comparison, he mentioned the specimen of *P. imitator* illustrated by Arkell (1958, pl. 26, fig. 3). Arkell’s specimen came from the Orbis Zone. Both *S. congener* and *P. imitator* have middle whorls similar to that of *Proplanulites*. *P. imitator* also has strong primary ribs and a less complex sutural pattern

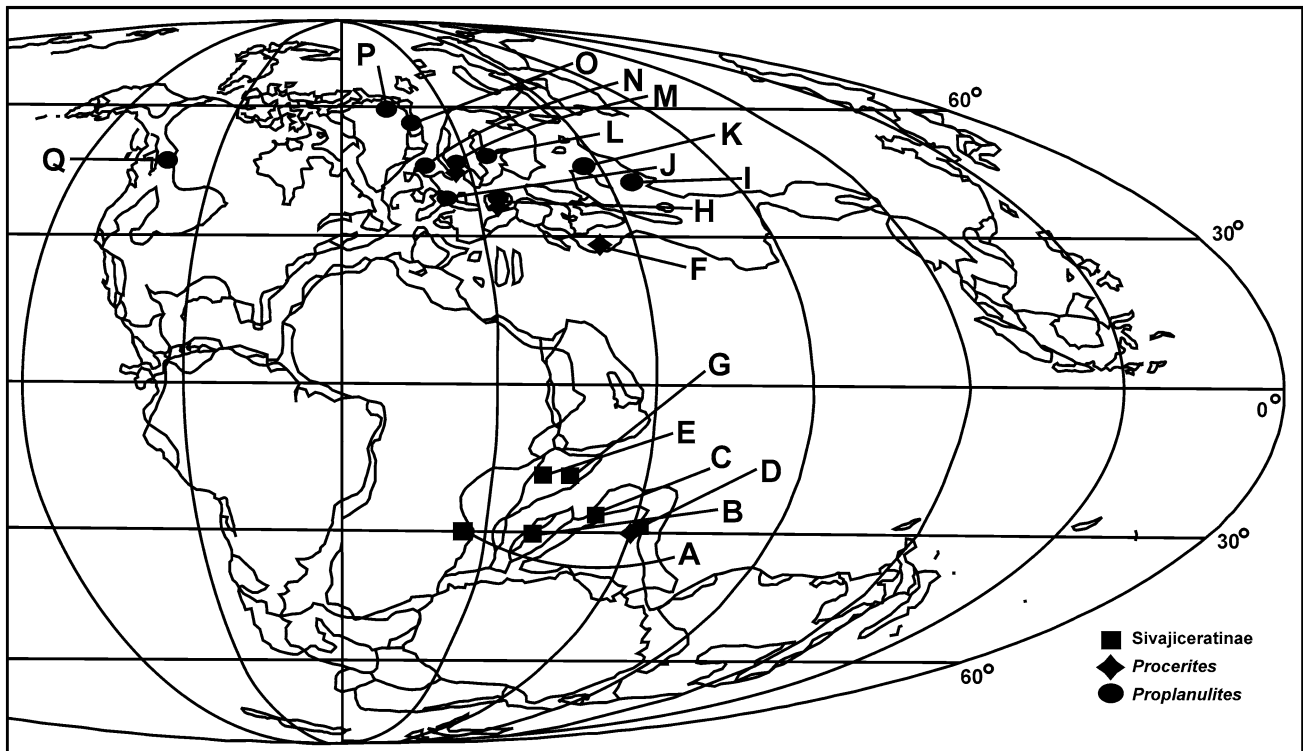


Fig. 19 Palaeobiogeographic distribution of Sivajiceratinae, *Procerites* and *Proplanulites* during the Bathonian–Callovian. Continental disposition is modified after Smith et al. (1994) and Bardhan et al. (2012). Note the distinct separation of the distribution of the Sivajiceratinae (Indo-Madagascan Province) and *Proplanulites* (Sub-boreal Europe). *Procerites* occurs in both biogeographic regions (main sources are Spath 1931; Arkell et al. 1957; Collignon 1958;

Imlay 1962; Hahn 1969; Cariou et al. 1996; Cariou and Hantzergue 1997; Pandey and Callomon 1995; Repin and Rashvan 1996a, b; Cariou and Enay 1999 and Gulyaev 2001); A Tanzania, B Madagascar, C Kutch, D Spiti, E Kenya, F Persia, G Somalia, H Caucasus, I Kazakhstan, J France, K Ukraine, L Poland, M Germany, N England, O Scotland, P Greenland, Q Canada

similar to *Proplanulites* (see Hahn 1969; pl. 4). Some *Procerites* species also have a smooth venter in the late stages of their ontogeny like that of *Proplanulites* (Bezanosov and Mikhailova, 1981; Gulyaev, pers. com., 2014).

It appears therefore *Procerites* might be the purported ancestor of *Proplanulites*. Admittedly, *Procerites* and *Proplanulites* have narrow, non-overlapping stratigraphic occurrences (see Fig. 20). According to Gulyaev (pers. com., 2014), the innermost whorls of *Proplanulites* bear a strong resemblance to the Pseudoperisphinctinae. But Callomon (1993) ruled out any connection between *Proplanulites* with the subfamily Pseudoperisphinctinae which is characterized by shorter secondary ribs dividing higher up on the whorl side. Moreover, Callomon (1993) emphasized the difference between the nature of dimorphism in both the groups. Gulyaev (pers.com.) found some transitional forms between the Pseudoperisphinctinae and the Proplanulitinae in Russia. But the forms appear to be very similar to the Pseudoperisphinctinae because of their evolute nature as well as weak and dense ribbing in the outer whorl.

A suggested line of phylogeny of the Sivajiceratinae n. subfam. and the Proplanulitinae from different species of *Procerites* is shown in Fig. 21. *Procerites* forms the ancestral genus. Sivajiceratinae n. subfam. and Proplanulitinae are the sister groups (see Smith 1994; Foote and Miller 2007). Both the subfamilies share synapomorphies like large, evolute shell, bullae-like primary ribs and adult smooth venter. Since they evolve from different stocks of *Procerites*, they have distinct autapomorphies. *Sivajicerata* retains the early ornamental features (strong and dense primary ribs) and complex suture of *Procerites hians*, while *Proplanulites* has less complex sutural pattern similar to that of *Procerites imitator*.

Procerites is older in Europe (middle Upper Bathonian). We here envisage that *Procerites* participated in a grand migrational event like many other ammonite genera and invaded the newly formed Kutch Basin during the Late Bathonian (Roy et al. 2007). It quickly speciated and gave rise to an endemic subfamily here described as the Sivajiceratinae n. subfam.

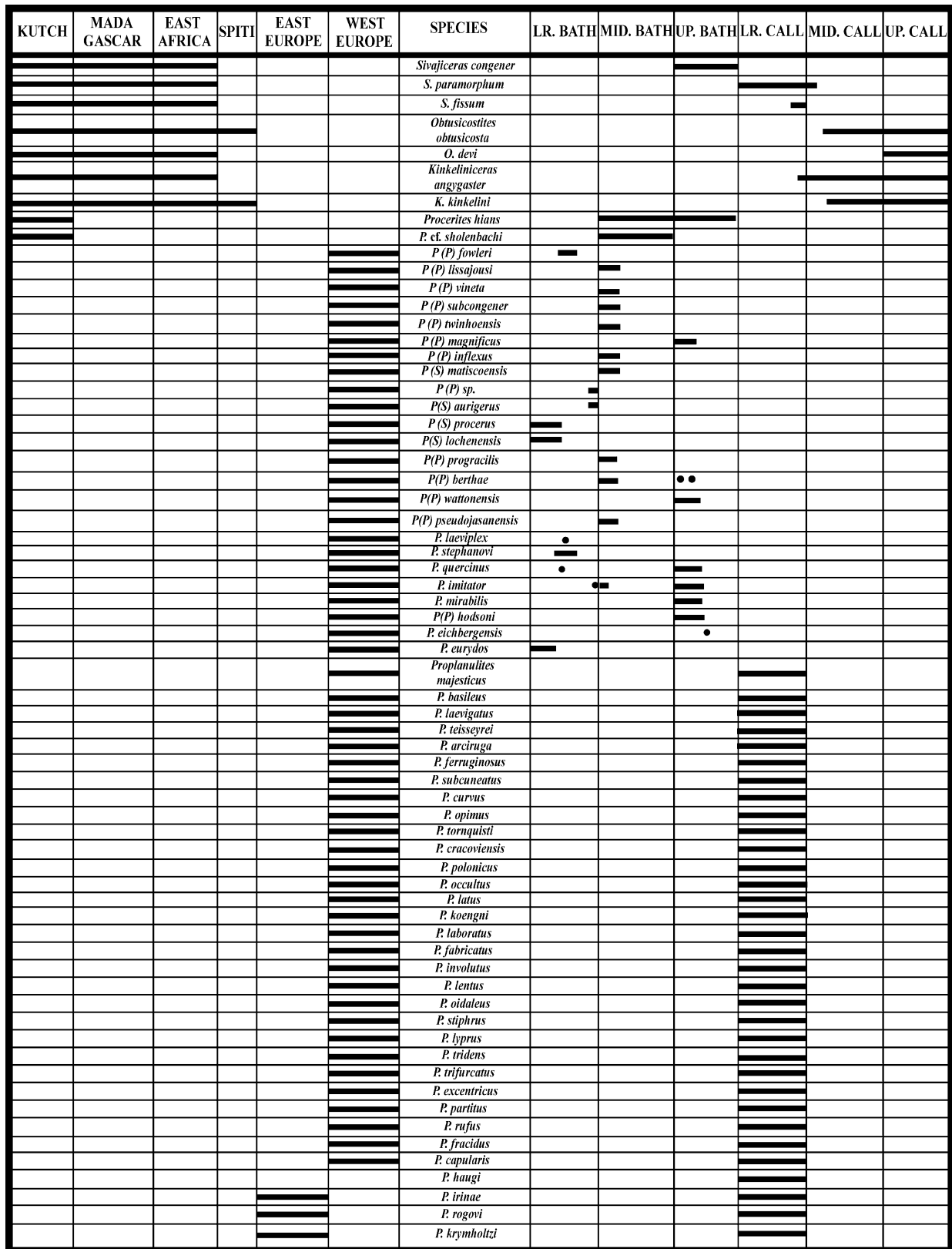


Fig. 20 Global stratigraphic and biogeographic distribution of members of the subfamily Sivajiceratinae, *Procerites* and *Proplanulites*. Sources are mentioned in Fig. 19

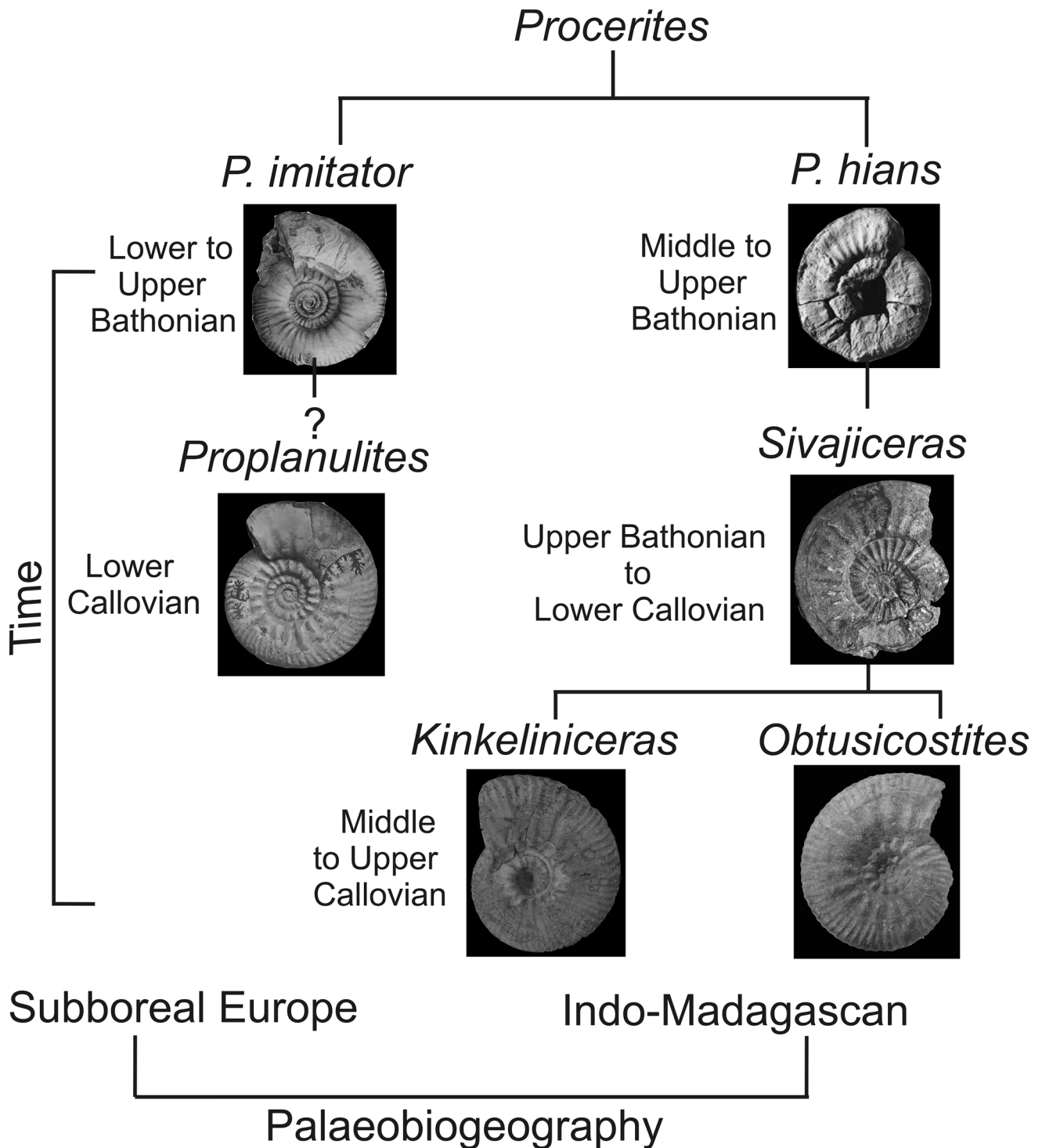


Fig. 21 Schematic diagram showing the probable evolutionary relationship among *Procerites*, *Proplanulites* and the subfamily Sivajiceratinae

Conclusions

Procerites is the ancestor of both *Proplanulites* of the Boreal and the Sivajiceratinae in the Indo-Madagascan Province. Sivajiceratinae evolved allopatrically when

Procerites invaded the Kutch sea. This is an example of allopatric mode of speciation. *Proplanulites* evolved from other stock of *Procerites* and flourished during the Lower Callovian in Europe. The stunning similarities between these two groups lie at their common ancestry.

Acknowledgments We thank the Director of the Repository Section of the Geological Survey of India for granting access to the GSI material. We thank A. Roy (Geological Survey of India, Kolkata, Lucknow, U.P.), Dr. Subhronil Mondal and Palaeontology laboratory members (Jadavpur University) for assistance in our research work. We also thank Dr. D. B. Gulyaev (Russia) for valuable discussion and providing important literature. We deeply acknowledge Zoe Hughes for various supports and Phil Hurst for the photography of the Department of Earth Sciences, Natural History Museum, U.K. Thanks are due to two anonymous reviewers and the guest editor, Dirk Fuchs of the Journal for their critical reviews and suggestions. We are especially indebted to the people of Jumara and Keera for their precious help during the field tours. S.B. received partial aid from the DST; CAS, Department of Geological Sciences; UPE-II, Jadavpur University, Kolkata. R.D. received partial aid from the UGC-BSR Scheme, Jadavpur University, Kolkata.

References

- Alberti, M., Pandey, D. K., Hethke, M., Fürsich, F. T., et al. (2015). Ammonites of the subfamily Mayaitinae Spath, 1928 from the Oxfordian of Kachchh, western India. *Geobios*, 48, 85–130.
- Arkell, W. J. (1958). *Monograph of the English Bathonian ammonites, Pt 7* (pp. 163–208). London: Monograph of the Palaeontographical Society.
- Arkell, W. J., Kummel, B., Wright, C. W., et al. (1957). Mesozoic Ammonoidea. In R. C. Moore & C. Teichert (Eds.), *Treatise on invertebrate paleontology. Part L. Mollusca* (pp. L80–L129). Boulder, CO: Geological Society of America and University of Kansas Press.
- Bardhan, S., Datta, K., Jana, S. K., Pramanik, D., et al. (1994). Dimorphism in *Kheraicerias* SPATH from the Callovian Chari Formation, Kutch, India. *Journal of Palaeontology*, 68, 287–293.
- Bardhan, S., Dutta, R., Chanda, P., Mallick, S., et al. (2012). Systematic revision and sexual dimorphism in *Hoffatia* (Ammonoidea: Perisphinctoidea) from the Callovian of Kutch, India. *Palaeoworld*, 21, 29–49.
- Beznosov, N. V., & Mikhailova, I. A. (1981). Systematics of Middle Jurassic leptosphinctins and zigzagiceratins. *Paleontological Journal*, 3, 47–60.
- Biswas, S. K. (1977). Mesozoic rock-stratigraphy of Kutch. *The Quarterly Journal of the Geological Mining and Metallurgical Society of India*, 49(3–4), 1–52.
- Biswas, S. K. (1982). Rift basins in the western margin of India and their hydrocarbon prospects with special reference to Kutch basin. *American Association of Petroleum Geologists Bulletin*, 66, 1497–1513.
- Biswas, S. K. (1991). Stratigraphy and sedimentary evolution of the Mesozoic basin of Kutch, Western India. In S. K. Tandon, C. C. Pant, & S. M. Casshyap (Eds.), *Sedimentary basins of India: Tectonic context* (pp. 74–103). Nainital: Gyanodaya Prakashan.
- Buckman, S. D. (1921). *Type ammonites* (Vol. III). London: William Wesley and Son.
- Callomon, J. H. (1993). On *Perisphinctes congener* Waagen, 1875 and the age of the Patchman Limestone in the Middle Jurassic of Jumara, Kutch, India. *Geologische Blätter für Nordost-Bayern*, 43, 227–246.
- Cariou, E., & Enay, R. (1999). The Bathonian–Callovian ammonites from Thakkhola (Central Népal): Biochronology and palaeobiogeographical aspects. *Geobios*, 32(5), 701–726.
- Cariou, E., Enay, R., Almeras, Y., et al. (1996). Newly discovered Callovian ammonite fauna in the Himalayan Spiti Shales at Spiti and compared chronostratigraphy of Middle and Upper Jurassic Succession in Spiti and Central Nepal (Thakkhola) areas. *Comptes Rendus de l'Académie des Sciences*, 332(IIa), 861–868.
- Cariou, E., & Hantzergue, P. (1997). *Biostratigraphie du Jurassique ouest-européen et méditerranéen: zonations parallèles et distribution des invertébrés et microfossiles*. Pau: Bulletin du Centre Recherche Elf, Exploration et Production, Mém.
- Collignon, M. (1958). *Atlas des fossils caractéristiques de Madagascar. Fasc II (Bathonian–Callovian)*. Tananarive: Service Géologique.
- Dacque, E., & Krenkel, E. (1909). Jura und Kreide in Ostafrika. *Neues Jahrbuch für Mineralogie, Geologie und Palaeontologie*, 28, 150–232.
- Datta, K. (1992). Facies, fauna and sequence: an integrated approach in the Jurassic Patcham and Chari Formations, Kutch, India. Ph.D. thesis, Jadavpur University, Kolkata, India.
- Foote, M., & Miller, A. I. (2007). *Principles of palaeontology* (3rd ed.). New York: W. H. Freeman and Company.
- Fürsich, F. T., Alberti, M., Pandey, D. K., et al. (2013). Stratigraphy and palaeoenvironments of the Jurassic rocks of Kachchh—Field Guide. *Beringeria, Special Issue*, 7, 1–174.
- Fürsich, F. T., & Oschmann, W. (1993). Shell beds as tools in basin analysis: The Jurassic of Kachchh, western India. *Journal of the Geological Society*, 150(1), 169–185.
- Fürsich, F. T., Oschmann, W., Pandey, D. K., Jaitly, A. K., Singh, I. B., Liu, C., et al. (2004). Palaeoecology of Middle to lower Upper Jurassic macrofaunas of the Kachchh Basin, western India: an overview. *Journal of the Palaeontological Society of India*, 49, 1–26.
- Fürsich, F. T., & Pandey, D. K. (2003). Sequence stratigraphic significance of sedimentary cycles and shell concentrations in the Upper Jurassic–Lower Cretaceous of Kutch, western India. *Palaeogeography, Palaeoclimatology, Palaeoecology*, 193, 285–309.
- Fürsich, F. T., Pandey, D. K., Callomon, J. H., Oschmann, W., Jaitly, A. K., et al. (1994). Contribution to the Jurassic of Kachchh, Western India. II. Bathonian stratigraphy and depositional environment of the Sadhara dome, Pachchham Island. *Beringeria*, 12, 95–125.
- Gulyaev, D. B. (2001). New ammonoids from the Subfamily Proplanulitinae Buckman from the Upper part of the Lower Callovian of Central Russia. *Palaeontological Journal*, 35(1), 18–22.
- Hahn, W. (1969). Die Perisphinctidae Steinmann (Ammonoidea) des Bathoniums (Brauner Jura) im südwestdeutschen Jura. *Jahreshefte des Geologischen Landesamtes Baden-Württemberg*, 11, 29–86.
- Imlay, R. W. (1962). Jurassic (Bathonian or Early Callovian) ammonites from Alaska and Montana. Geological Survey Professional Paper 374-C (pp. 1–32).
- Jana, S., Bardhan, S., Halder, K., et al. (2005). Eucycloceratin ammonites from the Callovian Chari formation, Kutch, India. *Palaeontology*, 48(4), 883–924.
- Jana, S., Bardhan, S., Sardar, S., et al. (2000). *Kheraicerias* Spath (Ammonoidea). New forms and records from the Middle Jurassic sequence of the Indian Subcontinent. *Paleontological Research*, 4(3), 205–225.
- Mitra, K. C., Bardhan, S., Bhattacharya, D., et al. (1979). A study of Mesozoic stratigraphy of Kutch, Gujarat with special reference to rock-stratigraphy and biostratigraphy of Keera dome. *Bulletin of Indian Geologists' Association*, 12, 129–143.
- Mukherjee, D. (2007). Taxonomic and phylogenetic study of Kutchithyris: A Jurassic terebratulide from Kutch, India. *Journal of Asian Earth Sciences*, 30(2), 213–237.
- Pandey, D. K., & Callomon, J. H. (1995). The Middle Bathonian ammonite families Clydoniceratidae and Perisphinctidae from Pachchham Island. *Beringeria*, 16, 125–145.

- Repin, Yu. S., & Rashvan, N. Kh. (1996a). Chronology and Chorology of the Callovian Ammonoids Mangyshlak. *Stratigraphy and Geological Correlation*, 4(5), 467–479.
- Repin, Yu. S., & Rashvan, N. Kh. (1996b). *Callovian ammonites of Saratov Povolzhye and Mangyshlak*. St Petersburg: Miri sem'ya-95.
- Roy, P., Bardhan, S., Mitra, A., Jana, S. K., et al. (2007). New Bathonian (Middle Jurassic) ammonite assemblages from Kutch, India. *Journal of Asian Earth Sciences*, 30, 629–651.
- Smith, A. B. (1994). *Systematics and the fossil record: documenting evolutionary patterns*. London: Blackwell Scientific Publications.
- Smith, A. G., Smith, D. G., Funnell, B. M., et al. (1994). *Atlas of Mesozoic and Cenozoic Coastlines*. Cambridge: Cambridge University Press.
- Spath, L. F. (1931). Revision of the Jurassic cephalopod fauna of Kachh (Cutch). *Palaeontologia Indica*, New Series 9, Memoir 2.
- Waagen, W. (1875). Jurassic Fauna of Kutch, the Cephalopoda. *Palaeontologia Indica*, New Series 9, Memoir 1.
- Westermann, G. E. G. (1966). Covariation and taxonomy of the Jurassic ammonite *Sonninia adicra* (Waagen). *Neues Jahrbuch für Geologie und Paläontologie Abhandlungen*, 124(3), 289–312.